DEVELOPMENT OF METHODOLOGIES TO ESTIMATE THE IMPACT OF OZONE ON VEGETATION

Contract EPG 1/3/104

FINAL CONTRACT REPORT; OCTOBER 2000

Prof. Mike Ashmore
Dr. Lisa Emberson
Dr. David Simpson
Dr. Juha-Pekka Tuovinen
Howard Cambridge

ACKNOWLEDGMENTS

We are indebted to the UK Department of the Environment, Transport and the Regions, the Scottish Executive, the National Assembly for Wales and the Department of the Environment in Northern Ireland for funding provided under contract No. EPG 1/3/104. The research has also been supported by funding from the Nordic Council of Ministers (NMR). The time spent by Dr. David Simpson and Dr. Juha-Pekka Tuovinen on the project was supported from the programmes of their own institutes (EMEP and Finnish Meteorological Institute respectively) on ozone deposition.

EXECUTIVE SUMMARY

- Ozone deposition to land surfaces across Europe depends to a large extent on the uptake of the pollutant through the stomata of surface vegetation. Surface deposition processes are an important component of the pan-European EMEP photochemical model that is currently used in risk assessment of ozone impacts and in assessing the impact of different ozone precursor control strategies within UN/ECE.

- The impacts of ozone on vegetation are more closely related to ozone flux through the stomata than to external concentrations. Therefore, a methodology based on predictions by the EMEP model of ozone flux, rather than the current AOT40 index, may provide a sounder basis for risk assessment of ozone impacts on vegetation across Europe.

- Stomatal conductance, and hence ozone flux to individual leaves and ozone deposition to land surfaces, is dependent on a number of environmental factors, such as irradiance, temperature, vapour pressure deficit, soil moisture deficit, as well as phenology.

- The current parameterisation of ozone deposition in the EMEP model is relatively simple, and no estimates are currently provided of stomatal ozone flux to vegetation. The key objective of this research project was to develop and test an improved deposition module for use in the EMEP model, which was designed to also allow predictions of stomatal ozone flux to be provided.

- This was accomplished by incorporating a model of stomatal conductance and ozone flux for different plant species, which had been developed by Dr. Emberson and Prof. Ashmore, into a deposition framework which could be applied in the EMEP model. This involved close collaboration with Dr. David Simpson at EMEP, and with Dr. Juha-Pekka Tuovinen, at the Finnish Meteorological Institute, who had been actively involved in developing deposition components of the EMEP model.

- This required a number of significant changes to the model structure and additional parameterisation. This report summarises these changes, describes the deposition patterns predicted by the model, assesses the performance of the model, and identifies the current uncertainties that remain.

- Conversion of the original stomatal conductance model to one capable of predicting total ozone deposition to vegetated surfaces necessitated the following modifications :- (i) allowing for ozone deposition to all sinks associated with vegetated surfaces; (ii) calculating ozone stomatal flux on a canopy scale rather than for an individual leaf; (iii) ensuring that parameterisations were available for all the major vegetation groups required to estimate the total deposition within all the EMEP grid squares across Europe.

- To enable preliminary deposition model runs, and subsequent analysis of results, a number of assumptions were necessary with regards to model parameterisation. The most important of these assumptions included (i) the use of fixed growing seasons for all vegetation groups; (ii) the application of fixed LAI parameterisation across Europe for each vegetation group and; (iii) the assumption that soil moisture is not limiting to stomatal conductance.

- These assumptions will need to be improved upon in the future as new data and techniques become available (e.g. application of growing season thermal time models, remote sensed data and soil moisture deficit models). Some work to assess the value of remote sensed data and to evaluate soil moisture deficit models was carried out in this research project.

- Preliminary deposition model runs were performed for four sites located across Europe - in Finland, Scotland, Switzerland and Portugal. These sites were selected mainly because of the availability of local field data for comparison. The results describe deposition velocity, canopy stomatal conductance and the influence of different environmental factors for six land-cover types.

- The results showed a strong seasonal variation in deposition velocity, with low values in winter and higher values in summer.

- The values of canopy conductance also showed strong seasonal variation and a strong diurnal variation, with higher values during the summer and mid-day periods. These canopy conductance values had a strong influence on the deposition values.

- Maximum canopy conductance values vary according to vegetation type, with the highest modelled values for grasslands and root crops resulting in high deposition velocities for these vegetation types. The maximum canopy conductances for the temperate coniferous group were lower by comparison; however, this group had high deposition velocities as a result of the low aerodynamic resistance associated with coniferous forests.

- In terms of total seasonal and annual deposition, the non-stomatal deposition pathways made a contribution of 50% or more for most locations and land cover types. The parameterisation of this component of the model is empirical and may need further attention. However, during mid-summer when ozone concentrations are generally higher, the stomatal pathway was found to be dominant in determining ozone deposition.

- For most land-cover types, temperature was found to cause the greatest limitation to stomatal deposition averaged over the year. Irradiance and phenology were also important but to a lesser extent.

- At all four locations, the aerodynamic and boundary layer resistances were small compared to canopy resistance for the temperate coniferous vegetation group. However, for short vegetation types (e.g. temperate cereals) the overall annual contribution of the sum of these two resistances to total resistance could approach 50%.

- Seasonal patterns in deposition velocity vary with geographical location. In Scotland and Switzerland annual profiles of deposition velocity (Vg) are similar with maximum values occurring in mid-summer. Vg values in Finland are lower and show a stronger seasonal variation whilst the Vg profile for Portugal shows two maxima, in the spring and autumn, with maximum values of Vg which are intermediate between Finland and the other two sites.

- The variations in canopy conductance indicate a clear contrast between the Portuguese location and the other three sites. In Switzerland, Scotland and in particular Finland, the lower values during the winter are due primarily to temperature limitations. In summer, vapour pressure deficit has a small effect in Switzerland and a strong effect at the Portuguese site. Temperature does not limit stomatal conductance at the Portuguese site in winter, but does have an effect in summer.

- Soil moisture deficit (SMD) was not included in these model runs due to uncertainty in both the method of derivation as well as the quality of the input climate data (from the new 50km version of the EMEP model). However, separate model runs conducted as part of the sensitivity analysis demonstrated the importance of the effect of SMD on forests, but not crops, especially in the later summer months at the Portuguese site.

- A separate evaluation of the performance of the SMD component of the model was performed for temperate cereal crops with i) a method devised by Mintz & Walker (1993) based on the simple water budget model first developed by Thornthwaite in 1948 and ii) with the MORECS SMD model used by the UK Meteorological Office.

- The SMD model provided predictions which were consistent with those of the MORECS model, and which appeared significantly better than those of the Mintz & Walker (1993) model.

- The model was then used to compare the simulated seasonal pattern of SMD in central England for different types of land-cover and the associated effect on stomatal conductance and ozone flux. The limiting influence of SMD on g_s was stronger for root crops and deciduous forests than for cereal crops and coniferous forests, with accumulated SMD being especially significant in July and August.

- The new SMD module appears to provide encouraging results. However, uncertainties still remain with its parameterisation for use in a pan-European model and in particular over the selection of appropriate values of rooting depth for different types of land-cover.

- Satellite remote sensed data provides information on spatial and seasonal variations in spectral signals from vegetation across Europe. Such data offers the potential to improve the parameterisation of LAI in the model.

- While such data may help in a qualitative sense to improve the parameterisation of LAI, a number of problems have been identified which mean that they cannot be used routinely to estimate LAI through standard algorithms. These problems include spatial matching of satellite data to land-cover types, saturation effects, and interference from cloud cover.

- The stomatal conductance of the canopy is calculated from data collected for individual leaves, using a model of the effect of increasing LAI on light extinction through the canopy. The simple algorithm used for this ‘canopy up-scaling’ contained certain assumptions that may not reflect all vegetation group characteristics as accurately as possible.

- The uncertainties associated with these assumptions were evaluated by running a stand-alone canopy up-scaling sub-model to identify the sensitivity of canopy conductance to the use of different extinction coefficients used to describe canopy architecture. This indicated that assigning vegetation-specific extinction coefficients could significantly improve the model for certain vegetation types.

- The "big leaf" method for up-scaling to the canopy level was tested for a range of LAI values (2 to 12 m^2/m^2) and it was found that this method was unable to correctly predict canopy conductance (G_{sto}) once maximum LAI values exceeded 6 m^2/m^2. The application of an "integrated" up-scaling approach, which is capable of calculating G_{sto} over a range of maximum LAI values, showed that significant increases in canopy conductance result from increases in LAI up to 12 m^2/m^2. However, it is apparent that as the LAI values increase the change in G_{sto} is reduced. This would suggest that the identification of correct LAI values between approximately 2 and 8 m^2/m^2 is more crucial than identification between say 8 and 12 m^2/m^2. The sensitivity of the "integrated" canopy up-scaling model to LAI was also found to vary throughout the year as a function of solar elevation.

- The performance of the deposition model has been evaluated through comparisons with published data in the literature, through direct comparisons with field data, and through sensitivity analysis.

- There are limited data available in the literature for comparison with model predictions. The model provided deposition velocity estimates that were broadly consistent with the range reported in the literature, although apparent over- and under-estimation was identified for specific types of land-cover.

- The model also appeared to predict adequately seasonal and diurnal patterns of deposition velocity, and the relative contribution of stomatal and non-stomatal components, except for the Mediterranean area, where the seasonal impact of soil moisture deficit on forests was not simulated.

- Comparisons have been made between model predictions and measured values of ozone deposition and stomatal flux in the field at certain sites. In making such comparisons, it is clear that a distinction needs to be drawn between the fact that the model parameterisation, designed for application across Europe, may not be appropriate for an individual field site.

- Once allowance has been made for local parameterisation, the model in general provides good agreement with field measurements of deposition and flux.

- There is some evidence from such comparisons that incorporation of additional factors (e.g. interactions between soil moisture deficit and vapour pressure deficit, and 'carry-over' effects of a previous year's drought) could improve model predictions of stomatal conductance.

- A sensitivity analysis of the model (which did include the influence of SMD on deposition) conducted for the four different locations across Europe, showed that predictions of deposition velocity were relatively insensitive to most specific components of the stomatal model. The exceptions, primarily for the southern site,

were soil moisture deficit and, to a lesser extent vapour pressure deficit. Furthermore, the limited sensitivity to temperature was due to counterbalancing of two stronger effects (a direct effect of low temperature and an indirect effect of high temperature through vapour pressure deficit). Scale effects on aerodynamic resistance and a strong effect of leaf area index (LAI) were also identified.

- The model predictions are sensitive to the assumed value of LAI. Improved agreement between model predictions and measurements have been obtained by using local LAI values rather than the default land-cover specific values used within the pan-European parameterisation of the model. The model formulation and parameterisation, together with a critical assessment of model performance and uncertainties, have been written as an EMEP note, and circulated to appropriate policy-makers and scientists.

- The research has been presented at meetings of ICP Modelling and Mapping and at meetings of ICP Vegetation, as well as at appropriate scientific meetings, to ensure that the development of the model and its implications for pan-European assessment of ozone effects, are regularly discussed within the UN/ECE framework.

In summary, this research project has succeeded in developing an improved and more mechanistic ozone deposition model for application within the EMEP model. This model also allows risk assessments for ozone impacts on vegetation to be based on stomatal ozone flux rather than AOT40.

The new model shows reasonable agreement with both primary field data and literature on ozone deposition. However, additional research is required to further test and improve the model, and to provide a stronger link to impacts on vegetation. Such improvements are essential to ensure that the model becomes an accepted tool for future assessments of ozone control policy within the UN/ECE framework.

TABLE OF CONTENTS

1. INTRODUCTION

1.1. Background

Ozone deposition to land surfaces across Europe depends to a large extent on the uptake of the pollutant through the stomata of surface vegetation. Surface deposition processes are an important component of the pan-European EMEP photochemical model that is currently used in risk assessment of ozone impacts and in assessing the impact of different ozone precursor control strategies within the UN/ECE. Furthermore, the impacts of ozone on vegetation are more closely related to ozone flux through the stomata than to external concentrations. The UN/ECE workshop on critical levels for ozone, held at Gerzensee, Switzerland in April 1999, recognised the need to move from the current Level I approach, based on the AOT40 index, to a Level II approach which is more closely related to the actual impacts of ozone on different types of vegetation and under different climatic conditions. Estimates of stomatal ozone flux would be an important element of such a Level II approach and therefore a methodology to predict stomatal ozone flux within the EMEP model would provide an essential tool for assessment of the impacts on vegetation of different ozone precursor control strategies.

The current parameterisation of ozone deposition in the EMEP model is relatively simple, and no estimates are provided of stomatal ozone flux to vegetation. The key objective of this research project was to develop and test an improved deposition module for use in the EMEP model, which was designed to also allow predictions to be made of stomatal ozone flux. This project involved close collaboration between Prof. Ashmore and Dr. Emberson, who had already developed a model of stomatal conductance and ozone flux for individual leaves, and Dr. Simpson, at EMEP, and Dr. Tuovinen, at the Finnish Meteorological Institute, who had developed the deposition components of the EMEP model. The effective collaboration with EMEP was also essential to ensure that the model could be readily incorporated into the overall EMEP photochemical model and hence could be applied directly in pan-European policy assessment.

This report covers research carried out over a period of 3 years, from October 1997 to September 2000. The original period of the contract was eighteen months to April 1999. Since then, the contract has been modified on a number of occasions to incorporate further research relating to the development and testing of the deposition model.

The initial contract specification initially focussed on improved assessment of the impacts of ozone in the U.K.. However, discussions with project officer at DETR, Dr. Duncan Johnstone, in the summer of 1998 indicated the much greater policy significance of improved assessments of ozone impacts on a European scale, especially given the international focus for policy development for control of ozone concentrations. In particular, the value of a strong operational link to the EMEP photochemical model was seen as of crucial importance, since this model is used to assess the effects of policy interventions on future ozone concentrations across Europe. This revised workplan was put into effect in October 1998, and has continued to provide the focus of the research over the subsequent two years, especially in view of the significance of developing tools for estimating ozone deposition across Europe. The earlier section of the research was described in the interim contract report, in October 1998, and therefore this report focuses on the development of the deposition/stomatal flux module for the EMEP model, which has been the prime focus of the subsequent research.

1.2 Report structure

Rather than provide a detailed report on all the work carried out in the course of this contract, this report summarises the main features of the work, outlines the key achievements, and assesses the policy implications. The detailed description of the work undertaken and the conclusions drawn is provided in the Annexe to this contract report, which contains detailed information in the form of peer-reviewed published papers, conference papers, reports, unpublished papers and project documents. These are referred to in the relevant sections of this summary report.

The most important and most recent of these projects output is the EMEP Note, which was published in August 2000. This Note, which is included in the Annexe, is of particular importance because it documents the key features of the model, describes the initial results of model runs, compares the model simulations with other measured and modelled deposition data, and assess the priorities for further development. The description of the results and model structure in the form of an EMEP note was designed to ensure widespread dissemination within the EMEP framework.

2. MODEL DEVELOPMENT

2.1 Introduction

The core of the model is a description of the responses of stomatal conductance and ozone flux through the stomata for a number of important European plant species under a range of environmental and other variables, as described by Emberson (1997). This core model only considers the stomatal resistance, and was initially extended, in a simplified format, under a previous DETR contract No. EPG 1/3/82, to enable the calculation of stomatal ozone uptake from ozone concentrations predicted by the EMEP photochemical model. The EMEP modelled ozone concentrations were at this time provided at a 150 x 150 km spatial scale at a height approximately 50 m above the ground surface. As such, it was necessary to calculate atmospheric (R_a) and boundary layer (R_b) resistances to ozone transfer to the height of the plant canopy and across the leaf boundary layer respectively before being able to calculate ozone flux to the sub-stomatal cavity as a function of stomatal conductance (g_s). However, these calculations ignore the fact that there are other ozone loss processes operating within a plant canopy, such as deposition to external plant surfaces or the ground. These will modify the ozone concentration gradient, meaning the simplified resistance pathway used in this version of the model will tend to overestimate the true stomatal flux of ozone.

Furthermore, one of the major shortcomings of the EMEP photochemical model was recognised to be the use of a fixed value of deposition velocity (0.5 cm s^{-1}) to describe ozone deposition to the vegetated surface (Simpson, 1996). The lack of vegetation- or environment- dependent descriptions of deposition velocity could lead to significant errors in the prediction of spatial and temporal variation in ozone deposition, and hence of ozone concentration, with obvious implications for pan-European policy evaluation. It is clear that inclusion of a more mechanistic stomatal ozone flux model could contribute significantly to resolving the problems of defining ozone deposition in a more mechanistic manner within the EMEP model. This was due to the fact that it has long been recognised that a major component of ozone deposition to vegetated surfaces is the stomatal uptake (e.g. Fowler et al. 1999). As such, a deposition model that incorporated a core biological

component differentiating between vegetation type, and including phenological and environmental components known to influence ozone deposition, should be capable of significantly improving the EMEP ozone deposition module. Furthermore, by using a more comprehensive deposition modelling scheme, the accuracy of modelled ozone flux into individual leaves could also be improved. Hence the key objectives of the model development which formed the central focus of the research project were to contribute to both improved modelling of ozone deposition and to the further development of methods of modelling ozone flux, and hence improving risk assessment for impacts of ozone across Europe.

A number of additions and modifications were necessary in order for the ozone stomatal flux model to be transformed into a model capable of predicting ozone deposition. The most important of these were :- (i) allowing for ozone deposition to all sinks associated with vegetated surfaces, i.e. not just ozone uptake to internal plant surfaces; (ii) calculating ozone stomatal flux on a canopy scale rather than for an individual leaf of the upper canopy; (iii) ensuring that parameterisation of the g_s model and additional deposition model parameterisation were available for species of all the major vegetation groups required to estimate the total deposition within all the EMEP grid squares across Europe. These additions and modifications are briefly described below with special reference to the variations from the original stomatal ozone flux model. A more comprehensive description of the deposition model formulation is detailed in the EMEP note given in the Annexe to this report (Emberson et al. 2000c).

2.2. Non-stomatal deposition

The primary non-stomatal sinks for ozone were identified from the literature as being the external plant parts (e.g. cuticles, bark, twig etc.) the ground surface underlying the vegetative canopy (including soil, litter moss etc.) and the associated in-canopy aerodynamic resistance to ozone transfer to this ground surface. The quantification of these additional ozone sinks is described in more detail in the EMEP note (Emberson et al., 2000c) in the report Annexe.

2.3 Calculation of Deposition Velocity

The total ozone deposition velocity (Vg m s^{-1}) was calculated according to a standard 3-resistance formulation. The resistances included atmospheric resistance (R_a) to mass transfer of ozone between the lowest part of the planetary boundary layer (approximately 50 m above surface), at which ozone concentrations are modelled by the EMEP photo-oxidant model, and the top of the canopy. Boundary layer resistance (R_b) to ozone diffusion across the quasi-laminar boundary layer close to the leaf surface. R_a and R_b are calculated according to Jakobsen *et al.* (1996). Finally, surface resistance (R_{sur}) to ozone deposition, which for vegetation classes is comprised of the plant canopy (described using a “big leaf” formulation) and the underlying soil, calculated as a simple multiple resistance. A graphical summary of the overall deposition scheme is given in Figure 2.1.

Figure 2.1 Resistance components included in the evaluation of ozone deposition to vegetated surfaces.

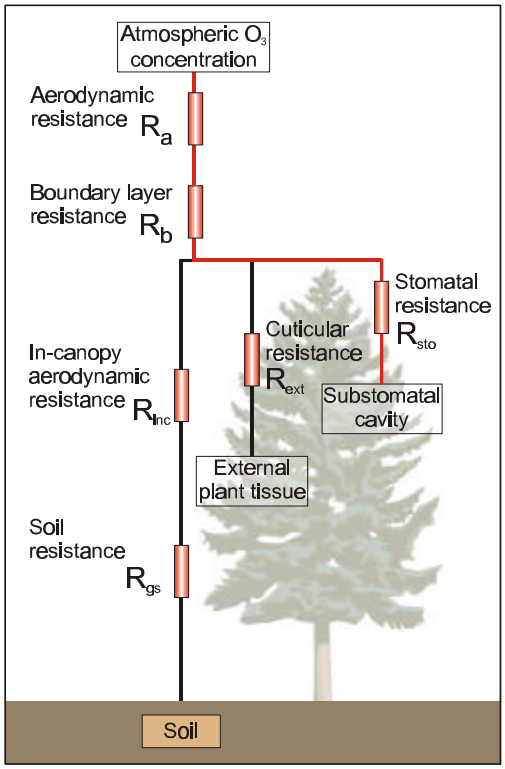

These stomatal and non-stomatal components of ozone deposition are combined to estimate the surface resistance to ozone deposition (Emberson et al., 2000c)

$$R_{sur} = \frac{1}{\frac{LAI}{R_{sto}} + \frac{SAI}{R_{e\,xt}} + \frac{1}{R_{inc} + R_{gs}}} \quad [1]$$

Where,

R_{sto} is the land-cover specific leaf/needle stomatal resistance (s m^{-1}), that is the resistance to ozone uptake through the stomata

R_{ext} is the external resistance (s m^{-1}) that is the resistance of the exterior plant parts to uptake or destruction of ozone

R_{inc} is the land-cover specific in-canopy aerodynamic resistance (s m^{-1}) that accounts for the resistance to transport of ozone within the canopy towards the soil and lower parts of the canopy

R_{gs} is the soil resistance (s m^{-1}) that accounts for the resistance to destruction or absorption at the ground surface (e.g. soil, litter, moss, etc.)

LAI is the leaf area index

SAI is a surface area index, set equal to LAI in the growing season and 1 outside the growing season when leaf material is not present

2.4. Canopy scale formulation

The original stomatal flux model calculated ozone uptake to a single leaf representative of those found in the upper layers of the vegetative canopy. To estimate ozone deposition, the ozone uptake to all leaves of the canopy needed to be evaluated. This required three

modifications to the original formulations :- (i) modifying the calculation of R_b to evaluate boundary layer resistance for the whole canopy rather than a single leaf of the upper canopy; (ii) using a radiation transfer model, together with values of Leaf Area Index (LAI) to scale up from the leaf to the canopy level; and (iii) allowing for the phenological effects on g_s for those species carrying needles of more than one age class (e.g. temperate coniferous species).

(i). Calculation of R_b

R_b (canopy boundary layer resistance) was calculated according to the standard EMEP deposition formulation as described in Jakobsen et al. (1996). This compared to the previous method of calculating r_b (single leaf boundary layer resistance) within the stomatal ozone flux model which used the method of Hosker (1986), which was specifically designed for individual leaves.

(ii) Calculation of canopy stomatal conductance

The use of LAI (defined as the leaf area per unit ground area) to scale up from the individual leaf to the canopy level allows ozone deposition to be described in terms of the unit area of ground covered by the canopy rather than per unit leaf area. Up-scaling of g_s from the leaf to the canopy is, however, not a just simple function of LAI since leaf / needle g_s varies within the canopy. This variation exists for a number of different reasons including leaf type (e.g. sun or shade leaf), canopy micro-climate and leaf age. Given the large numbers of vegetation groups for which parameterisation is needed, it was not considered feasible at this stage to incorporate all of these factors in a model of canopy conductance. Instead, irradiance (which is considered to be the most dominant determinant of g_s variation within a plant canopy) was the only factor included in the up-scaling calculation. The effect of irradiance on canopy conductance was assessed by calculating the effect of direct and diffuse irradiance on the g_s of sunlit and shaded portions of the canopy using the core stomatal conductance model. The radiation transfer within the canopy, was calculated according to a method devised by Norman (1982), that estimates diffuse and direct irradiance on sunlit and shaded leaves / needles within vegetative canopies. This method was modified to treat the canopy as a “big leaf”. The formulations used to calculate irradiance at the top of the canopy are those of Jakobsen et al. (1996); i.e. the same methods used in other EMEP gaseous deposition models.

(iii) Inclusion of phenological component

The g_s of leaves and needles decreases with age. For those vegetation groups whose canopies comprise of leaves/needles that emerge and senesce within a single year the phenological component of the core stomatal ozone flux model accounts for the variability in g_s with age within a single year. However, for certain vegetation groups, namely the needle bearing forest groups (temperate coniferous and Mediterranean needle types), needles remain on the tree for a number of years. Since these older needles comprise a significant proportion of the total canopy leaf area, the effect of needle age on canopy conductance needs to be incorporated into the model for these vegetation groups. A method was developed to incorporate the effect of needle age for coniferous temperate forests and was applied in the calculations of ozone deposition for this land-cover type. This method divides the canopy LAI into two needle classes, varying this ratio throughout the year as appropriate for the phenology of this cover type. Appropriate values for the g_s of these two needle classes were also selected from the literature and again varied

annually. The effect of incorporating this phenological component into calculations of canopy conductance is described in Figure 2.2. where the original calculation method is plotted along with the "needle age" method. Figure 2.2 shows that the inclusion of the variability in g_s with needle age results in a significant decrease in canopy conductance over most of the year. Further details of the method are detailed in the EMEP note (Emberson et al. 2000c).

Figure 2.2 Canopy conductance (G_{sto} mmol O_3 m^{-2} s^{-1}) as a function of canopy radiation and needle age for the coniferous temperate forests cover type. G_{sto} given as midday values for each month assuming cloudless conditions.

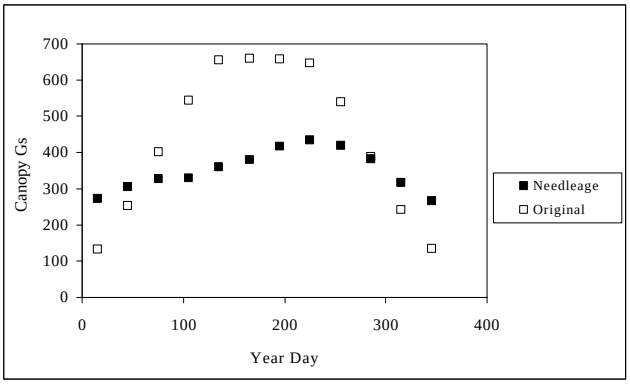

3. MODEL PARAMETERISATION

3.1. Introduction

In order for the model to accurately predict ozone flux or deposition, a wide range of input data are required. A particular challenge in modelling pan-European deposition, as opposed to stomatal flux to individual leaves, is the need to integrate the values across a range of vegetation types within each grid square. This means that parameterisation is required for all land covers across the EMEP modelling domain, rather than for individual species of concern in terms of ozone impacts.

A key tension in this pan-European model is therefore between providing sufficient detail in the model to allow the key features of ozone deposition across Europe to be simulated, and being able to provide a parameterisation for an array of model terms for all major vegetation types. In this section, we describe the key elements of the parameterisation for the additional terms that were required to adapt the core stomatal conductance model to form the current deposition model. The parameterisation of the stomatal conductance model itself is described elsewhere (see Emberson et al., 2000c in the Annexe). We have also identified certain aspects of the model parameterisation which are particularly complex but to which model predictions are highly sensitive. In the final two parts of this section, we describe more detailed analysis of the model inputs for two of these problem areas of parameterisation – leaf area index (LAI) and soil moisture deficit (SMD).

3.2 Meteorological and ozone concentration data

The EMEP model within which this deposition model will be installed and which provides the ozone concentration data for the preliminary deposition model runs performed within this study, is a pan-European 3-D model with 20 vertical layers and a horizontal resolution

of approximately 50 x 50 km^2 (Jonson et al., 1999). The meteorological data for this model has a 3 hourly resolution and is provided by a dedicated version of a Numerical Weather Prediction (NWP) model (Sandnes, Lenschow and Tsyro, 2000).

3.3 Land Cover Parameterisation

The core stomatal conductance (g_s) model described variation in g_s in response to four environmental variables (irradiance, temperature, VPD and SMD). This model had already been previously parameterised for important individual species. However, the deposition model required two further developments of this parameterisation to account for the fact that deposition was modelled for major land cover classes, rather than for individual species. Firstly, it has been necessary to identify land cover classes which comprise species with similar characteristics in terms of aerodynamic resistance and stomatal conductance characteristics, and hence to pool the existing data for individual species. Secondly, the g_s database in the core stomatal model has been significantly expanded, by extraction of data from the literature for as many species as possible within each land cover class (although complete parameterisation of the g_s model for all four environmental parameters was only possible for a limited number of species).

For certain land cover classes, it was not possible to obtain adequate data to parameterise the stomatal conductance model. In such cases, instead, an empirical description of the surface resistance has been used for these land cover classes. Table 3.1 gives the main land-cover classes in the deposition model, along with an indication of whether a bulk-surface resistance or stomatal modelling approach is used. For those land cover classes for which a stomatal modelling approach was used, the key species used to parameterise the stomatal model are listed.

For forest trees, the vegetation groupings include species for which a complete g_s model parameterisation was available and which are representative of some of the more common and hence widespread European species. In addition to modelling deposition to broad forest categories, it is also possible for us to model stomatal flux to the individual species listed in Table 3.1. For arable crops, the situation is rather different, largely because of the limited data available for mapping the distribution of crop species, as opposed to arable land, across Europe. The most frequently occurring crop species are wheat, barley and maize. Of these crops, a complete g_s parameterisation only exists for wheat and maize. Therefore, for deposition modelling, wheat g_s parameters are used to characterise temperate crop species and maize g_s parameters to characterise Mediterranean crop types. Root crops have also been treated as a separate class based upon data existing for potato.

Moorlands and heathlands have been treated somewhat differently. The variable mix of species present, and the lack of g_s data in the literature, has meant that we have adopted an empirical approach, based on deposition studies. This approach uses a modified version of stomatal conductance modelling in which g_{VPD} and g_{SWP} are excluded from the calculation (in effect this means that it is assumed that VPD and SWP will not limit ozone uptake via the stomata in these ecosystems). The parameterisation of g_{age}, g_{min} and g_{light} is based on that collected for grasslands whilst g_{temp} is assumed similar to temperate/boreal coniferous forest. The value of g_{max} was assigned so as to produce model results in accordance with published deposition velocities for this land-cover type.

For tundra and wetlands, no useful stomatal data could be found and therefore a simple parameterisation of the surface resistance was used. Finally, the deposition velocity for the

four non-vegetated surfaces was the same as in previous versions of the EMEP model. The detailed parameterisation used for all these land cover classes is summarised in the EMEP note (Emberson et al., 2000c) in the Annexe.

Table 3.1. Land-cover classes chosen for deposition calculations and representative species for which stomatal conductance (g_s) data were available. A "Y" in the g_s column indicates classes for which stomatal conductance modelling is performed.

Code	Deposition Land-class	g_s	Representative species (for which g_S data were available)
CF	Temp./boreal coniferous forests	Y	Norway Spruce (*Picea abies*), Scots Pine (*Pinus sylvestris*)
DF	Temp./boreal deciduous forests.	Y	Oaks (*Quercus petraea Q. robur*), Beech (*Fagus sylvatica*), Birch (*Betula pendula*)
NF	Medit. Needleleaf forests	Y	Allepo pine (*Pinus halepensis*), Maritime pine (*Pinus pinaster*), *Abies* spp.
BF	Medit. Broadleaf forests	Y	Oaks (*Q. ilex, Q. suber, Q. coccifera*)
TC	Temp. crops	Y	Wheat (*Triticum aestivum*)
MC	Med. Crops	Y	Maize (*Zea Mays*)
RC	Root crops	Y	Potato (*Solanum tuberosum*)
V	Vineyards	Y	Grapevine (*Vitis vinifera*)
TO	Temp. orchard	Y	Apple (*Malus sylvestris*)
MO	Med. Orchard	Y	Citrus (*Citrus sinensis & C. paradisi*)
GR	Grassland	Y	*Lolium* spp.
SNL	Semi-natural	Y*	Moor/heathland*
MS	Med. Scrub	Y	*Q. ilex*
WE	Wetlands	-	
TU	Tundra	.	
DE	Desert	.	
W	Water	.	
I	Ice	.	
U	Urban	.	

* Empirical approach – see text above

3.4 Land Cover Maps

The SEI land cover map has been used extensively within this research project for modelling ozone uptake over Europe. The original land cover map (Figure 3.1) covered most of Europe and was appropriate for European mapping over the geographic extent covered by the coarse 150 x 150 km scale climatic data. However, the 50 x 50 km grid for routine modelling carried out by EMEP extends the coverage further east to include further areas of Russia. Land cover datasets of this extended coverage in the detail required for deposition modelling are unavailable from other sources, and therefore it was necessary to update the existing SEI-Y land cover within the GIS in the course of this project.

The original SEI European Land Cover data set was created by combining information from a variety of existing digital and mapped sources. The distribution of European tree species was derived by combining two data sources:- the distribution of tree cover for Europe (ESA, 1992), which describes the presence or absence of forests at a 1 km^2

resolution for the early 1990s, and the distribution of deciduous, coniferous and mixed woodland forest types, which was digitised from FAO-Cartographia, (1980), which describes the distribution of land-cover types for Europe in the 1970s. Also described by FAO-Cartographia (1980) are the distributions of orchards and vineyards. The digitised FAO-Cartographia (1980) map was also used to classify European agricultural areas, and then were combined with information on areas for which statistical information describing yield data for various crops have been compiled (Eurostat, 1994) to assign the dominant crop type to each agricultural area. For countries outside the European Union (EU), agricultural statistics from AGRISTAT database were used (FAO-Agristat, 1990), which describe dominant crop types at an international level.

To extend the coverage of the land cover map to include eastern Russia maps of the former USSR ("Land Use Map of the Former USSR", at 1:4000000, 1991, CCCP, Moscow) were identified which were of suitable scale, spatial coverage and classification. The legends for the map were translated from Russian into English and these hard copy paper maps were then digitised by SEI-Y and combined with the original land cover datasets to produce final map shown in Figure 3.2. The nominal resolution of the map has been determined to be 1:5000000. The complete map is divided in to 90 dominant cover types. It is important note that this map may have wider application to other deposition modelling or risk assessment methods within the UN/ECE framework

3.5 Modelling and parameterisation used for preliminary model analysis

At the present time there are some components of the modelling and land-cover schemes that are in the process of being developed. The most important modelling problem concerns soil-water, and as noted previously we confine this report to the study of well-watered vegetation, with $g_{SWP}=1$. For land-cover, work is still needed to define LAI and its seasonal variation in an optimal way. However, it is considered that the bulk of this deposition module is now far enough evolved to provide preliminary model outputs to be produced and tested against existing measured data. The assumptions that have been used in conjunction with the model components that are still under development will, in the near future, be tested and where appropriate improved, so that these components can eventually be incorporated into the overall deposition module.

The following section describes the methods currently being used to calculate these model components still under development which include a) estimation of growing season; b) estimation of leaf area index and c) methods used to up-scale from the leaf/needle to the entire canopy. These descriptions are included so as to give a complete documentation of the methods used to achieve the preliminary model results. These results are described and compared with measured data, collected either from published papers or available (but as yet unpublished) data from field campaigns.

Figure 3.1. The original SEI Land Cover Map (pre 1999)

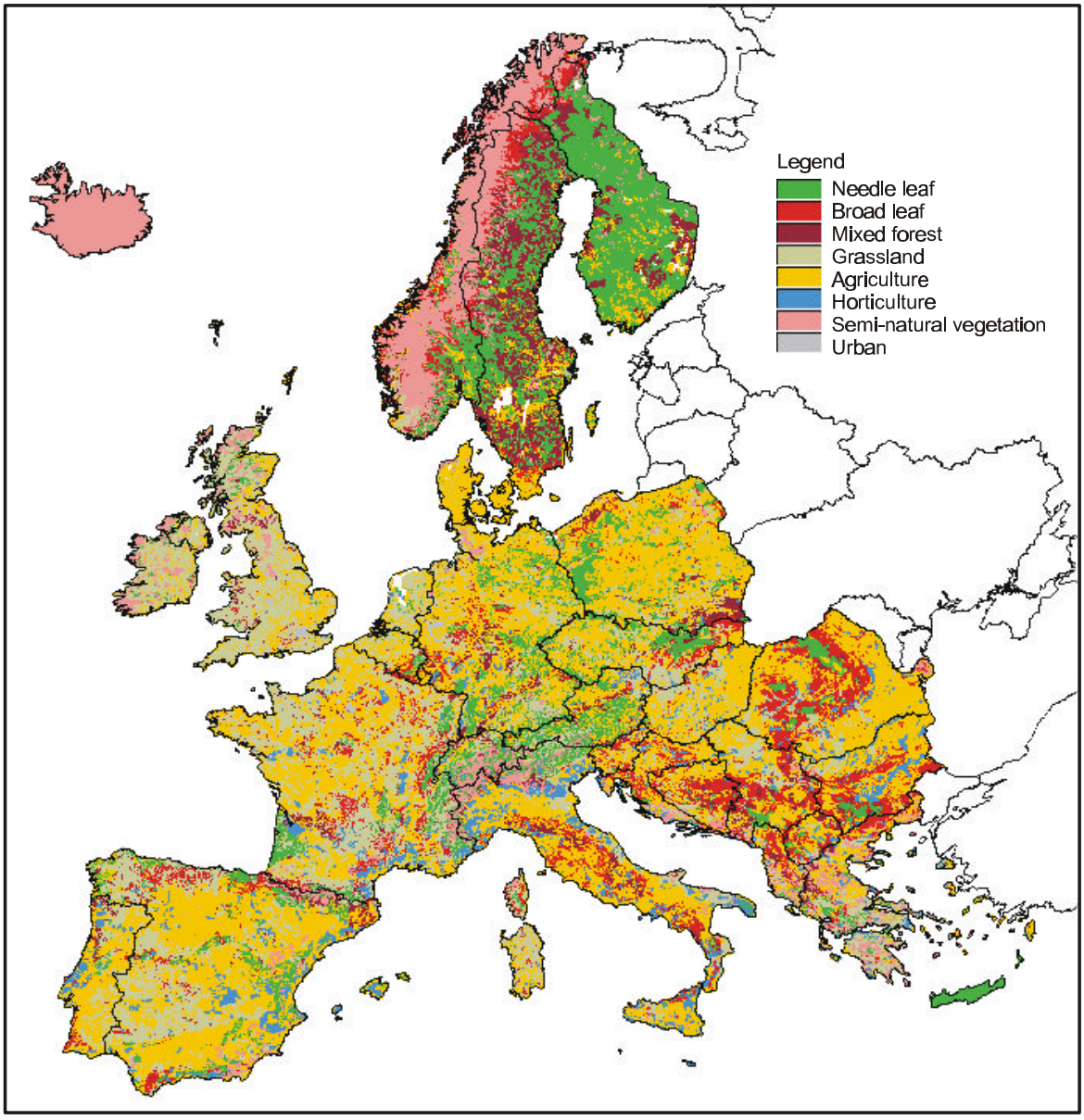

Figure 3.2. The revised SEI Land cover including Russia and former Russian states.

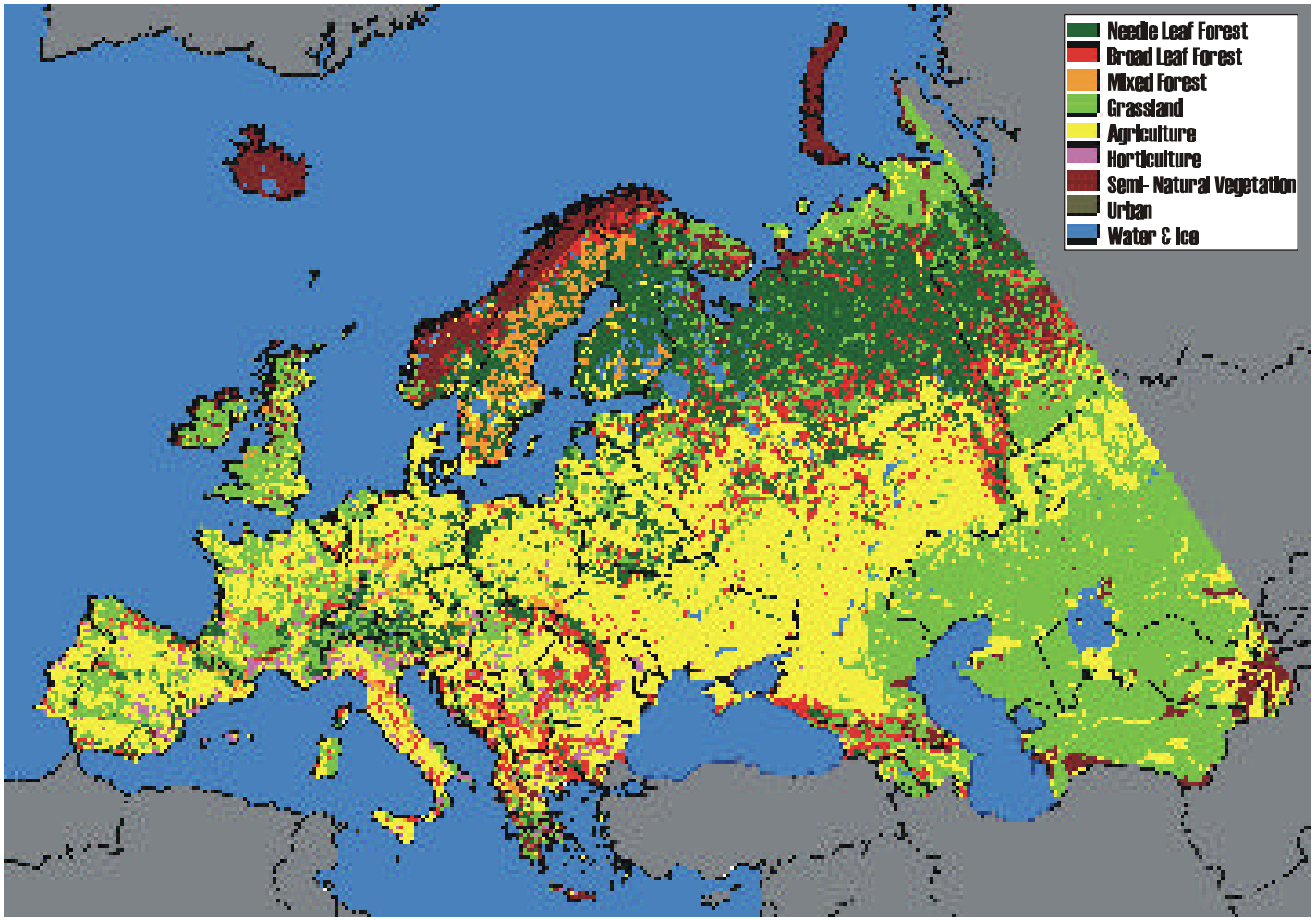

3.6 Growing season

The growing season is defined as that part of the year when the leaves are physiologically active and hence allowing significant ozone uptake. Of the land-cover types considered in this study, only the temperate/boreal coniferous forests, moorlands/heathlands and grasslands will have needle or leaf areas outside the period of the growing season. During this period it is assumed that R_{sto} will be equal to $(g_{min} / 41000)^{-1}$ (Körner, 1994). For all other land-cover types, either the leaves are not present (LAI=0) or the growing season is assumed to continue throughout the year. The Surface Area Index (SAI), which allows for the fact that the woody plant material will still provide a significant sink to ozone deposition after senescence, is included only for deciduous forests. SAI is set equal to LAI in the growing season for these forests, or to 1 m^2 /m^2 outside the growing season.

The model runs described in Section 4 used fixed growing season length and timings based upon published studies that have documented such data. The fixed dates used for each land-cover type are shown in Table 3.2. Although the use of a fixed growing season is not ideal, it does give an indication of the variability in length and timing of growing seasons and hence the seasonal differences in ozone deposition between the individual land-cover types. In the future, thermal time models, which estimate growing seasons according to land-cover type specific temperature sum thresholds will be investigated. These should generate a more realistic spatial distribution of both growing season and LAI changes, as well as allowing year-to-year variation due to climatic factors to be incorporated in the model simulations.

Table 3.2 Start (SGS) and end (EGS) dates (day numbers) of fixed growing seasons used for model comparisons

Land-cover Class	SGS	EGS	References
Temp./boreal coniferous	0	365	Körner (1995)
$*g_{age}$	0	485	Beadle *et al.* (1982)
Temp./boreal deciduous	90	270	Abdulla & Lettenmaier (1997), Olson *et al.* (1985), Padro (1996), Jakobsen et al. (1996)
Medit. Needleleaf	0	365	Hassika et al. (1997)
Medit. Broadleaf forests	0	365	Sala & Tenhunen (1994), Gratani (1993), Sala & Tenhunen (1996)
Temp. crops	105	197	Olson *et al.* (1985), Boumann (1995)
Med. Crops	150	300	Studeto et al. (1995), Bouman (1995)
Root crops	130	250	Pers. comm. Vandemeiren (EU CHIP Project)
Vineyards	120	300	Padro (1994), Mascart *et al.* (1991)
Temp. orchard	90	270	Tustin et al. (1988); Palmer et al. (1992)
Medit. Orchard	0	365	Padro (1994), Mascart *et al.* (1991)
Grasslands	0	365	Mascart *et al.* (1991), Olson *et al.* (1985)
Semi-natural	0	365	Mascart *et al.* (1991), Olson *et al.* (1985)
Med. Scrub	0	365	Pio et al. (2000)

N.B. The Temp./boreal coniferous forest group has two different parameterisation. The second parameterisation ($*g_{age}$) is used in conjunction with the methodology to estimate the canopy conductance according to needle age. The EGS of 485 enables the use of the generic g_{age} calculation incorporating the fact that the current year needles are assumed to emerge on 1st April and then become "older" needles on 1st April of the following year. Note that the references in this table are given in the Annexe of the EMEP note (Emberson et al., 2000c).

3.7 Leaf Area Index; Model Parameterisation

For the model runs described in Section 4, values of LAI were assigned to each land-cover, according to the functions plotted in Figure 3.3. Table 3.3 summarises the parameter values used for each of the different land-cover types. The parameterisation is based on defining a minimum and maximum value of LAI for each land cover, and a seasonal variation that is consistent with the definition of the growing seasons. The values used were derived from published data collected from the literature for representative species of each land-cover type.

Table 3.3 Maximum LAI and course of LAI throughout the growing season for the different land-cover categories.

Land-cover Class	SLAI	ELAI	LAI_min	LAI_max	SLAI_len	ELAI_len	References
Temp./boreal coniferous forest	0	365	3.4	4.5	192	96	Abdulla & Lettenmaier (1997), Neilson & Marks (1994), Beadle *et al.* (1982)
Temp./boreal deciduous forest	=SGS	=EGS	3.5	5	56	92	Abdulla & Lettenmaier (1997), *Olson et al.* (1985), Padro (1996), Jakobsen et al. (1996)
Medit. Needleleaf forests	0	365	-	3.5	-	-	Hassika et al. (1997)
Medit. Broadleaf forests	0	365	-	4.5	-	-	Sala & Tenhunen (1994), Gratani (1993), Sala & Tenhunen (1996)
Temp. crops	=SGS	=EGS	0	5	70	22	Olson *et al.* (1985), Boumann (1995)
Med. Crops	=SGS	=EGS	0	3.5	70	44	Studeto et al. (1995), Bouman (1995)
Root crops	=SGS	=EGS	0	6	35	65	Pers. comm. Vandemeiren (EU CHIP Project)
Vineyards	0	365	-	3	-	-	Padro (1994), Mascart *et al.* (1991)
Temp. orchard	=SGS	=SGS	1	3.5	60	100	Tustin et al. (1988); Palmer et al. (1992)
Medit. Orchard	0	365	-	3	-	-	Padro (1994), Mascart *et al.* (1991)
Grasslands	0	365	2	5.5	140	135	Mascart *et al.* (1991), Olson *et al.* (1985)
Moor/heathland	0	365	2	5	192	96	Abdulla & Lettenmaier (1997), Neilson & Marks (1994)
Med. Scrub	0	365	-	4.5	-	-	Pio et al. (2000)

Note that the references listed in this table are given in the Annexe of the EMEP note (Emberson et al., 2000c).

Figure 3.3 Generic function for Leaf Area Index (LAI) and examples of seasonal course of LAI for selected land-cover types.

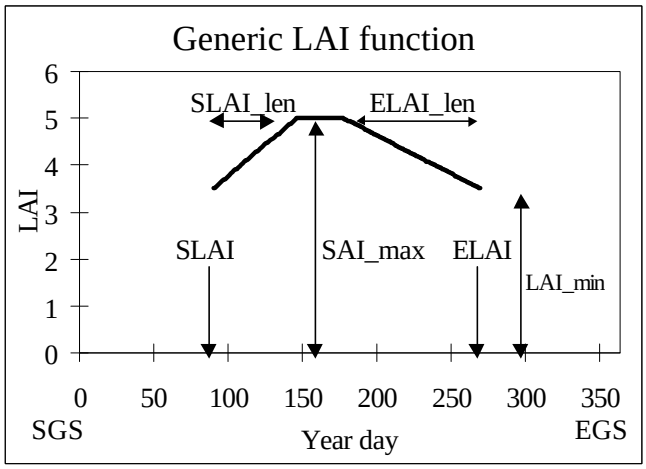

The model uses stomatal conductance collected from individual leaves to predict canopy conductance, using a simple method of correcting for the effects of increasing light extinction with increasing leaf area index (LAI). To assess whether this simple model leads to errors in the prediction of canopy conductance, a simple sub-model was developed and applied. The results of this work are described in a separate "canopy up-scaling" project report. A summary of the most important factors related to this up-scaling technique that were found to influence model predictions of canopy conductance are presented below.

3.7.1 Methodology used to upscale from leaf to canopy

The core stomatal conductance model calculates g_s for an individual young fully developed leaf or needle. To calculate the canopy conductance it is necessary to scale up from the leaf/needle to the canopy level. The preliminary model runs resulting in the outputs presented in Section 4 were achieved by calculating g_{light} according to the appropriate visible radiation value as it varies with cumulative LAI within the canopy. The radiation transfer within the canopy is calculated according to the method devised by Norman (1982) as presented in Baldocchi et al. (1987), that estimates diffuse and direct irradiance on sunlit and shaded leaves/needles within vegetative canopies. The calculations of direct (I_{dir}) and diffuse (I_{diff}) solar irradiance (W m^{-2}) and solar elevation ($\sin\beta$) are made according to Jakobsen et al. (1996) where $\sin\beta$ is the complement of the zenith angle of the sun. Note that I_{dir} and I_{diff} are converted from W m^{-2} to μmol m^{-2} s^{-1} by multiplying by 4.57 for use within the following equations.

The sunlit leaf area (LAI_{sun}) of the canopy is calculated according to: -

$$LAI_{sun} = (1 - \exp(-ks * LAI)) / ks \quad [2]$$

Where *ks* is equal to $1 / 2\sin\beta$. The proportion of the total LAI that is shaded (LAI_{shade}) is then simply calculated as: -

$$LAI_{shade} = LAI - LAI_{sun} \quad [3]$$

PAR_{sun}, which is dependant on the mean angle between leaves and the sun, is calculated using a modified "big leaf" version of the canopy radiation transfer model of Norman (1982) where the flux density of PAR on sunlit leaves is: -

$$PAR_{sun} = I_{dir} * \cos(\theta) / \sin\beta + PAR_{shade} \quad [4]$$

Where I_{dir} is the flux density of direct PAR above the canopy and θ is the angle between a leaf and the sun. For these calculations it is assumed that the canopy has a spherical leaf inclination distribution (θ) constant at 60 degrees.

PAR_{shade} is calculated semi-empirically by: -

$$PAR_{shade} = I_{diff} * \exp(-0.5 * LAI^{0.7}) + 0.07 * I_{dir} * (1.1 - 0.1 * LAI) * \exp[-\sin\beta] \quad [5]$$

.
The calculation of the g_{light} values is performed as previously for the core stomatal conductance model (Emberson et al., 2000c) for both sunlit and shaded leaves which are weighted according to the fraction of sunlit (g_{light}sun) and shaded (g_{light}shade) respectively. These g_{light} values are summed to give the total irradiance-dependant canopy conductance (g_{light}). This method has been simplified so that rather than integrating g_{light} over the canopy a "big leaf" approach has been employed. This means that g_{light} will be underestimated since the model does not allow for the variability in direct and diffuse irradiance within the canopy. However, since these parameters vary only slightly the model under-estimations, when LAI values are < 6 m^2/m^2 are relatively small.

$$g_{light}sun = [1 - \exp(-\alpha * PAR_{sun})] \quad [6]$$

$$g_{light}shade = [1 - \exp(-\alpha * PAR_{shade})] \quad [7]$$

Finally, g_{light} is calculated as: -

$$g_{light} = g_{light}sun * LAI_{sun} / LAI + g_{light}shade * LAI_{shade} / LAI \quad [8]$$

This mean canopy g_{light} value is used in the core stomatal conductance equation to calculate mean canopy leaf/needle conductance (G_{sto}). The inverse of G_{sto} (i.e. canopy resistance or R_{sto}) is then used in equation [1] in combination with the cover-type specific LAI to upscale from the leaf/needle to the canopy level.

3.7.2 Extinction Co-efficients

The method described above assumes that the leaves within the canopy have a spherical leaf orientation distribution (θ) constant at 60 degrees. This assumption means that the penetration of irradiance into the canopy is also dependant on the solar elevation (β), as such, the definition of the extinction co-efficient (*ks*) has been written to involve β where *ks* is equal to 1 / (2sin β). However, it is acknowledged that the assumption of a spherical leaf orientation type may not be appropriate for all deposition land-cover. Observed *ks* values have been found to vary from 0.3 to 1.5 dependent upon factors such as species and stand type (Jones, 1992). Values less than 1 are obtained for non-horizontal leaves or clumped leaf distributions, while values greater than 1 occur with horizontal leaves of a

more regular arrangement in space. Extinction co-efficients that have been suggested for certain leaf angle distributions and measured for real canopies are described in Table 3.4

Table 3.4 Extinction co-efficients for model and real canopies (cf. Monteith & Unsworth, 1990)

Idealized leaf angle distribution	Extinction co-efficient (*ks*)
Horizontal	1
Vertical	$(2\cot\beta)/\pi$
Spherical	$1/(2\sin\beta)$

It should be noted that the *ks* for the idealized leaf distributions are written to involve the solar elevation term (β). This has the advantage of describing irradiance within the canopy as a function of beam elevation as well as leaf angle distribution and was the method used by Baldocchi et al. (1987) where the *ks* for an assumed spherical canopy was written as $1/(2\sin\beta)$.

Model runs were performed using a stand-alone Excel model to determine canopy conductance sensitivity to different *ks* values for coniferous temperate species and temperate cereal species. The results are shown in Figures 3.4 and 3.5 below.

Figure 3.4 Effect on canopy conductance (mmol O_3 m^{-2} s^{-1}) of varying extinction co-efficients for coniferous temperate species. Calculations are made for solar noon at latitude 56°N.

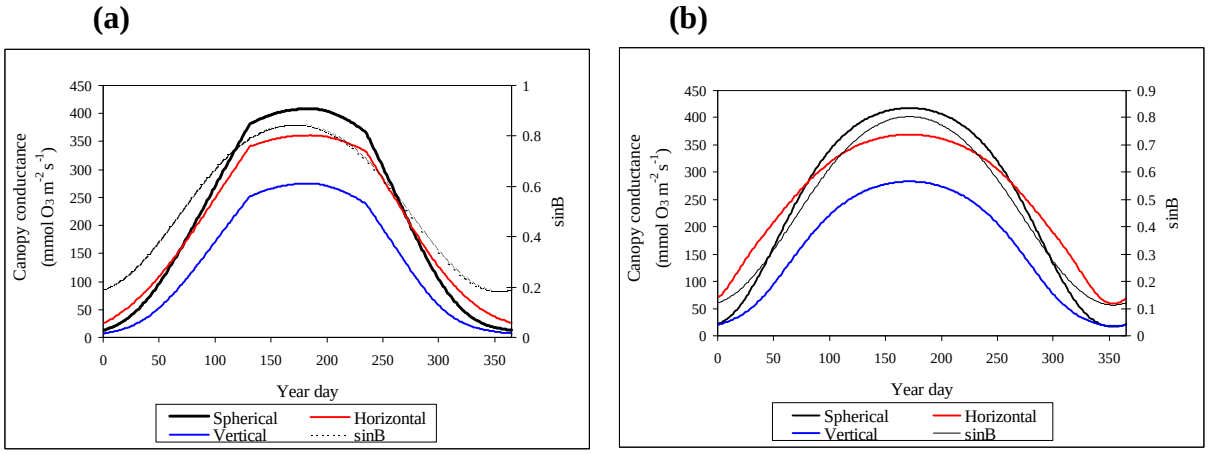

Figures 3.4 and 3.5 show two situations for each vegetation type. The first (graph (a)) describes the effect of altering the extinction co-efficient on an "actual" canopy conductance i.e. allowing for growing season and associated change in LAI and g_{max} with phenology assuming optimum conditions for g_s. The second (graph (b)) describes the variation in canopy conductance assuming a constant and maximum LAI and g_{max}. This graph is included to aid the interpretation of results and hence enable the effect of varying extinction co-efficients for other vegetation groups to be inferred.

Figure 3.5 Effect on canopy conductance (mmol O_3 m^{-2} s^{-1}) of varying extinction co-efficients for temperate cereals. Calculations are made for solar noon at latitude 56°N.

(a) **(b)**

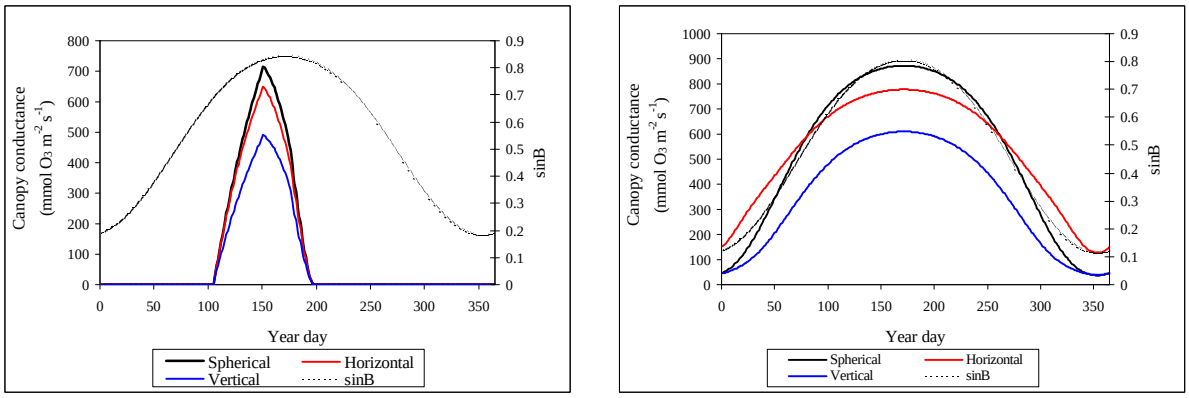

It is clear from both vegetation types graph (a) that the choice of extinction co-efficient can significantly affect the estimated canopy conductance. The vertical leaf arrangement results in the lowest canopy conductance throughout the year, this is due to vertical leaves having a lower level of irradiance per unit surface area. The difference in canopy conductance is reduced at the start and end of the year as the solar elevation is lower (i.e. the sun is lower in the sky) and hence the angle between the sun and the leaf is closer to a perpendicular. The difference between the spherical and horizontal leaf distribution on canopy conductance varies over the course of the year. The horizontal distribution results in greater conductance both at the start and end of the growing seasons whilst the spherical distribution seems to be the optimum for irradiance capture during the middle of the year. The horizontal distribution performs better during the winter months since all leaves of the outer canopy are equally exposed to irradiation, for the spherical distribution many of the outer canopy leaves will not be receiving any direct irradiance to the upper leaf surface. During the summer, the horizontal arrangement performs less well as irradiance is not able to penetrate the canopy to the degree that is possible under the spherical arrangement.

The results show that selecting an appropriate extinction co-efficient for each vegetation type is crucial. At present, all vegetation types are assumed to have a spherical leaf orientation, however, the leaf angle distribution of cereal crops is probably closer to the vertical distribution pattern and as such the current model is likely to be over predicting canopy conductance, at least during mid-day periods. Further research needs to be performed to indicate which leaf angle distribution is most appropriate for use with the different needle bearing vegetation groups taking into account needle clumping as well as orientation.

3.7.3 Sensitivity to LAI Parameterisation

Using appropriate LAI parameterisation is crucial to ensuring accurate calculations of canopy conductance as will be shown in the assessment of the model performance presented in Section 5.2 and 5.3 where the differences between observed and modelled values were on many occasions associated with over or under predictions in LAI.

The up-scaling described in this report has been performed using a “big leaf” approach where the canopy is represented by a single leaf layer and conductance is calculated

according to input parameters representing the whole canopy (e.g. direct and diffuse irradiance values calculated after transmission through the entire canopy). This simplified approach to canopy up-scaling gives reasonably accurate results within the range of default LAI values (i.e LAI ≤ 6) used in the preliminary ozone deposition model runs presented in this report. However, as is described in Section 3.8 it is recognised that there is likely to be significant variability in LAI values within vegetation groups across Europe. Such variations will be larger for certain vegetation types such as the temperate coniferous species where LAIs have been reported to range from 2.5 m^2/m^2 (e.g. Tuovinen, 1999) to > 10 m^2/m^2 (e.g. Coe et al. 1995). In view of this, the simplified "big leaf" up-scaling model was tested against the more computational intensive "integrated" up-scaling model (as described in Baldocchi et al., 1987 and shown below in equation 9) to assess the relative abilities to estimate canopy conductance over a range of LAI values. The results of this assessment are described in Figure 3.6 where the calculations are made for a latitude of 56°N for the coniferous temperate vegetation type.

$$G_{sto} = \int_0^f dF_{sun}(f) * g_{light}[PAR_{sun}(f)] + dF_{shade}(f) * g_{light}[PAR_{shade}(f)]df \qquad [9]$$

Where G_{sto} is the canopy stomatal conductance; F is the leaf area, dF_{sun} and dF_{shade} are the differences in sunlit and shaded leaf areas respectively between F and $F+dF$ and PAR_{sun} and PAR_{shade} are the direct and diffuse irradiance values in μmol m^{-2} s^{-1} on sunlit and shaded leaves respectively. This equation is evaluated for differences in F dF of 0.25 to minimize the influence of leaf overlap.

Figure 3.6 Canopy conductance (G_{sto}) values calculated using the "big leaf" (BL) and "Integrated" (I) up-scaling methods for mid January and July assuming maximum LAI values of 2, 4, 6, 8, 10 and 12.

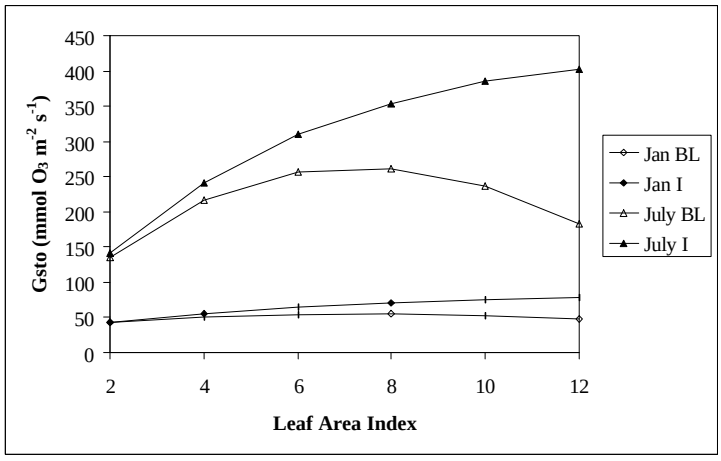

The graph shown in Figure 3.6 describe model runs that have been performed to indicate the sensitivity of calculated canopy conductances of temperate coniferous forests to LAI parameterisation i.e. using a maximum LAI value (LAI_max) value different to the current model default value of 4.5 m^2/m^2. These model runs include the phenological variation in LAI and g_{age} over the growing season, all other factors are assumed not-limiting (e.g. irradiance, temperature, VPD and SMD) to canopy conductance. To sensibly vary the LAI parameterisation it was necessary to vary the minimum LAI (LAI_min) values in proportion to the change in the LAI_max value. This was achieved by maintaining a

constant ratio between LAI_max and LAI_min so that LAI_min is always 0.77 times LAI_max.

Figure 3.6 shows that the "big leaf" approach underestimates canopy conductance, and that for specific situations (when irradiance at the top of the canopy is high) increases in LAI of greater than 6 m^2/m^2 will result in decreases in G_{sto}. These results are incorrect and increase in LAI should always result in an increase in G_{sto} although the relationship between the two parameters is not linear. These inaccuracies are a result of the "big leaf" model being unable to describe the complex interactions between the distribution of shade leaves and the associated diffuse radiation intensities in distinct canopy layers. Canopy conductances using the integrated approach evaluate the g_s of sun and shade leaves for distinct layers of leaf areas equal to 0.25 using the appropriate direct or indirect irradiance values for sun and shade leaves respectively. In contrast the "big leaf" method uses the cumulative value of sun or shade LAI (i.e. the whole canopy ratio of sun and shade leaves) and the corresponding direct of diffuse irradiance value (i.e. the irradiance levels that have been transmitted through the canopy). It is this method of calculating the shade leaves contribution to whole canopy conductance that results in inaccuracies since the reduction in diffuse irradiance levels with transmission through the canopy is within the range of g_s response between relative g_{min} and g_{max}. As such, the shade leaves of the middle canopy layers (up to a cumulative LAI of about 4) are those that contribute most of all the shade leaves to the total canopy conductance. This is because it is in these layers that significant numbers of shade leaves are present and where levels of diffuse irradiance are high enough to induce significant stomatal opening. At higher levels in the canopy too few shade leaves are present to contribute significantly to G_{sto} whilst at lower canopy levels the diffuse irradiance levels are too low to allow shade leaves to add significantly to G_{sto}. This situation is described in Figure 3.7 which shows the proportions of g_{light}sun and g_{light}shade within each discrete canopy layer (where, for example, g_{light}shade is a function of the diffuse irradiance and the shade leaf area in that layer) of a canopy of LAI = 12.

Figure 3.7 The proportions of g_{light}sun and g_{light}shade within each discrete canopy layer. Calculations made assuming direct and diffuse irradiances of (a) 40 and 10 W/m^2 and (b) 360 and 40 W/m^2.

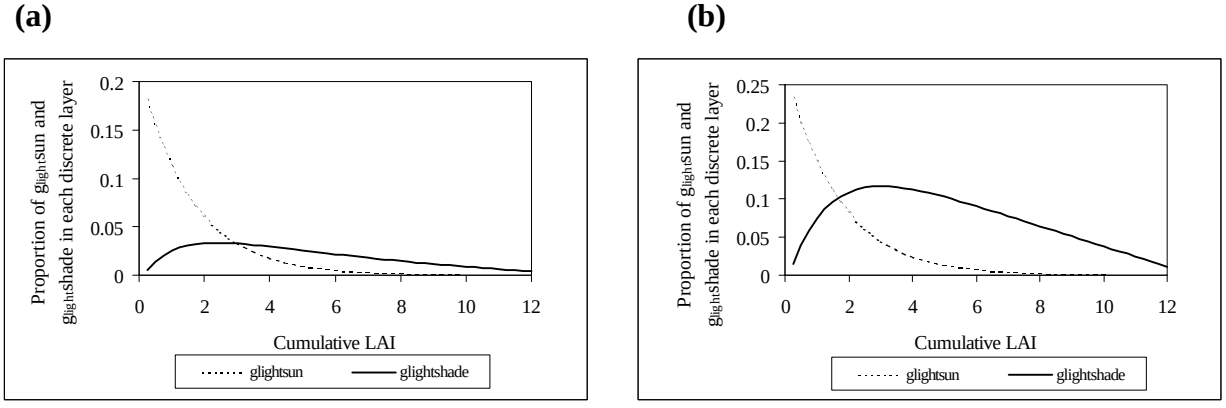

Figure 3.7 clearly describes how the inaccuracies of the "big leaf" method increase as irradiance increases. In graph (a) the diffuse irradiance at the top of the canopy is of such a low value that there is little difference between the contribution to overall canopy conductance of the shade leaves at different heights within the canopy. However, as the values of irradiance increase, as shown in graph (b), the significantly enhanced

contribution of the shade leaves contained in the leaf layers up to a cumulative leaf area of about 4 is quite apparent. The decrease in the relative contribution of the shade leaves g_s to G_{sto} is reflected in Figure 3.6 at a LAI of approximately 4 m^2/m^2 where the "big leaf" and "integrated" G_{sto} values initially start to diverge.

This modelling work has highlighted two important points. Firstly, that the "big leaf" method for up-scaling to the canopy level should not be used once parameterisation of maximum LAI values exceeds 6 m^2/m^2. Secondly, the application of the "integrated" up-scaling approach shows that significant increases in canopy conductance result from increases in LAI up to 12 m^2/m^2. However, it is apparent that as the LAI values increase the change in G_{sto} is reduced. This would suggest that the identification of correct LAI values between approximately 2 and 8 m^2/m^2 is more important than similarly correct identification between 8 and 12 m^2/m^2.

In summary, the selection of an appropriate LAI value is crucial to the calculation of canopy conductance. The sensitivity of the model to LAI varies throughout the year as dictated by solar elevation. It should also be pointed out that the calculation of g_{age} for the temperate coniferous vegetation type (which in this instance calculates canopy conductance as a function of the different age classes present within the canopy) assumes a specific proportion of current to older (i.e. > 1 year old) needle age classes over the year. Skärby et al. (1995) showed that the proportions of current to older needles present on Norway spruce trees decreased with age; 8 year old trees (with an LAI of 2) were compared with 89 year old trees (with an LAI of 10) and estimated that current year needles made up 72% and 16% respectively of the canopy. This variability in needle age class proportions will need to be taken into account once it is possible to describe the European variation in LAI within cover types.

3.8 Leaf Area Index: Satellite data

One alternative source of information that could be used to provide input data on LAI is satellite imagery. While it is uncertain that satellite imagery could provide the appropriate information, the lack of alternative sources of pan-European data made it important to critically assess the potential value of this approach. Therefore, in the final phase of the contract, we examined the potential of one such dataset to determine the spatial and temporal variation in LAI across Europe. The results of this assessment are presented in detail in the Annexe, in the form of a project report. The key features of this report are summarised here.

It has been previously proposed that LAI can be derived from the Normalised Difference Vegetation Index (NDVI) which is regularly produced as satellite data output from the Advanced Very High Resolution Radiometer (AVHRR), the principal sensor on board the series of Polar Orbiting Environmental Satellites operated by NOAA. The magnitude of NDVI is generally related to the level of photosynthetic activity in the observed vegetation. The range of values varies from 0 to 1 where higher values of NDVI indicate greater vigour and amounts of vegetation. NDVI is a combination of radiances and reflectances in different spectral channels. It is considered to be proportionate to ground plant biomass, green leaf biomass and absorbed photosynthetic active radiation and is calculated according to equation [10].

$$NDVI = (Near\ Infrared - Visible) / (Near\ Infrared + Visible) \qquad [10]$$

The temporal and spatial coverage of the NOAA AVHRR sensor coupled with its appropriate spectral resolution enables NDVI to be calculated on a 6 hourly basis at spatial scales of 1, 4 and 15 km depending on the desired product.

The following procedure, documented in Sellers et al. (1994) for use in atmospheric circulation models, has been adapted to investigate whether LAI can be modelled with sufficient accuracy across Europe for use in deposition models. The following steps were employed in the calculation to produce weekly and monthly estimates of LAI over Europe.

i) Selection of training sites within homogenous cover types across Europe. Three dominant cover types were identifiable on the SEI Land Cover Map and visible on the NDVI satellite imagery. These were an agriculture class (assumed to be wheat), a broadleaf vegetation type and a needleleaf vegetation type. As it was not possible to overlay the land cover map with the satellite data within the GIS, there is uncertainty in associating the satellite image with a particular land cover that needs to be considered when interpreting the results described below.
ii) Monthly NDVI profiles were extracted for these sites from satellite imagery for 1996 and 1997. Weekly profiles were also extracted for 1996 only. These are presented in the accompanying diagrams. Global one degree data were also extracted for comparison purposes.
iii) FPAR was calculated based on relationships presented in Sellers et al. (1994). Fraction of Absorbed Photosynthetic Active Radiation (FPAR) value is described as the radiation utilisable by the plant for growth and is near-linearly related to LAI.
iv) Finally, LAI was calculated from FPAR using functions for crops and broadleaf vegetation defined by Montieth and Unsworth (1990) and for needleleaf by Goward and Huemmrich (1992).

Figure 3.8 shows the raw NDVI data across Europe for five months during 1996. The maps show the clear seasonal patterns of vegetation growth, and the large spatial gradients across Europe, especially in the winter.

Figure 3.8 Raw NDVI data across Europe for five months during 1996

February **April** **June**

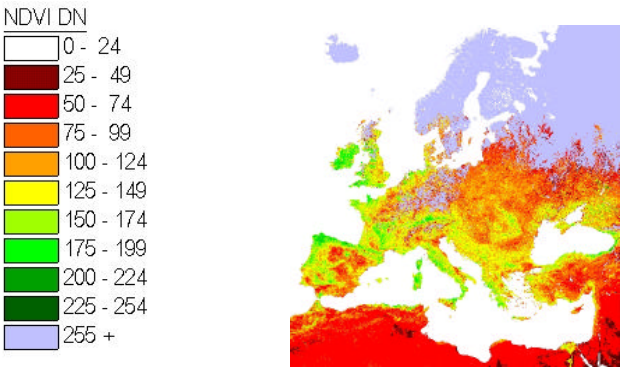

July **Legend** **November**

The monthly (Figure 3.9 (a-d)) and weekly (Figure 3.10 (a-d)) profiles of LAI show the results obtained by applying the algorithms to specific locations across Europe with different dominant vegetation types. Figures 3.9a and 3.10a compare monthly profiles over both 1995 & 1996; and weekly profiles over 1996 respectively for two sites classified on the SEI-Y land cover maps as needleleaf vegetation. These sites are located in Northern Finland and Austria and clearly show a marked seasonal variation which is stronger than expected for this vegetation type. The marked seasonality shown by the profiles could be due to several factors influencing the signal received by the sensors. For example, the contribution of snow-cover or the influence of soil moisture on the signal received by the sensor can have the affect of reducing overall reflectance.

The profiles in Figures 3.9b and 3.10b for broadleaf trees found in Spain (beech) and Italy (oak), in contrast, show little variation over the year. This might be expected for Mediterranean evergreen oaks, but is unexpected for beech; it is possible that the problems of matching the NDVI and land-cover datasets meant that other types of vegetation were present. The profiles in Figures 3.9c and d, and in Figures 3.10c and d, relate to wheat in four different locations. The LAI profiles illustrated in Figures 3.9c (describing wheat LAI in Italy and the UK) and 3.10c (describing wheat LAI in Spain) show a more gradual decline in LAI for wheat than the expected rapid decrease in LAI following the onset of senescence and then marked decrease as it is harvested. However, Figure 3.10d (describing wheat LAI in the Czech Republic and Germany) does shows a more characteristic profile for wheat, with a much greater seasonal variation, including a sharp increase in the spring.

Figure 3.9 Monthly LAI profiles during 1996 and 1997 for (a). Needleleaf in Finland and Austria; (b) Broadleaf in Italy and Spain; (c) Wheat in Italy and UK; and (d) Wheat in Czech Republic and France.

(a) **(b)**

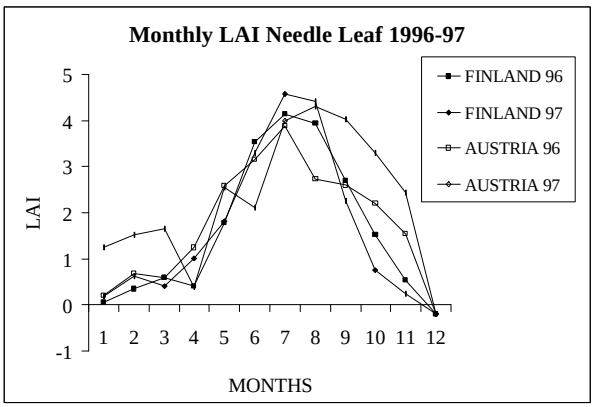

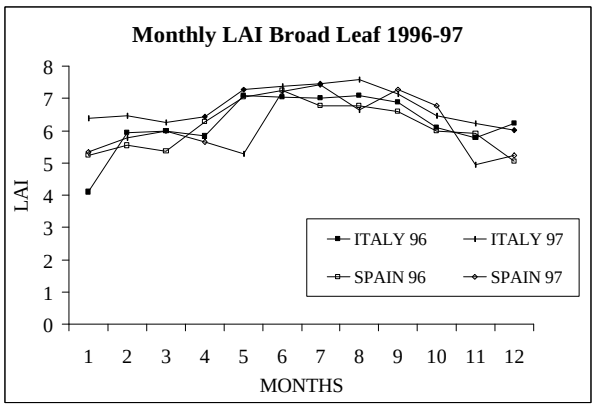

(c) **(d)**

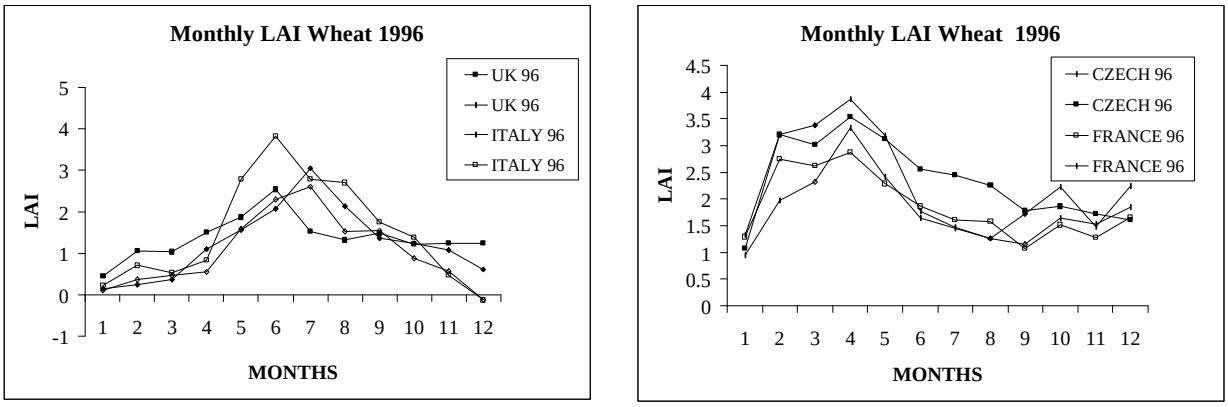

Figure 3.10 Weekly LAI profiles during 1996 for (a). Needleleaf in Finland and Austria; (b) Broadleaf in Italy and Spain; (c) Wheat in Spain and (d) Wheat in Czech and Germany.

(a) **(b)**

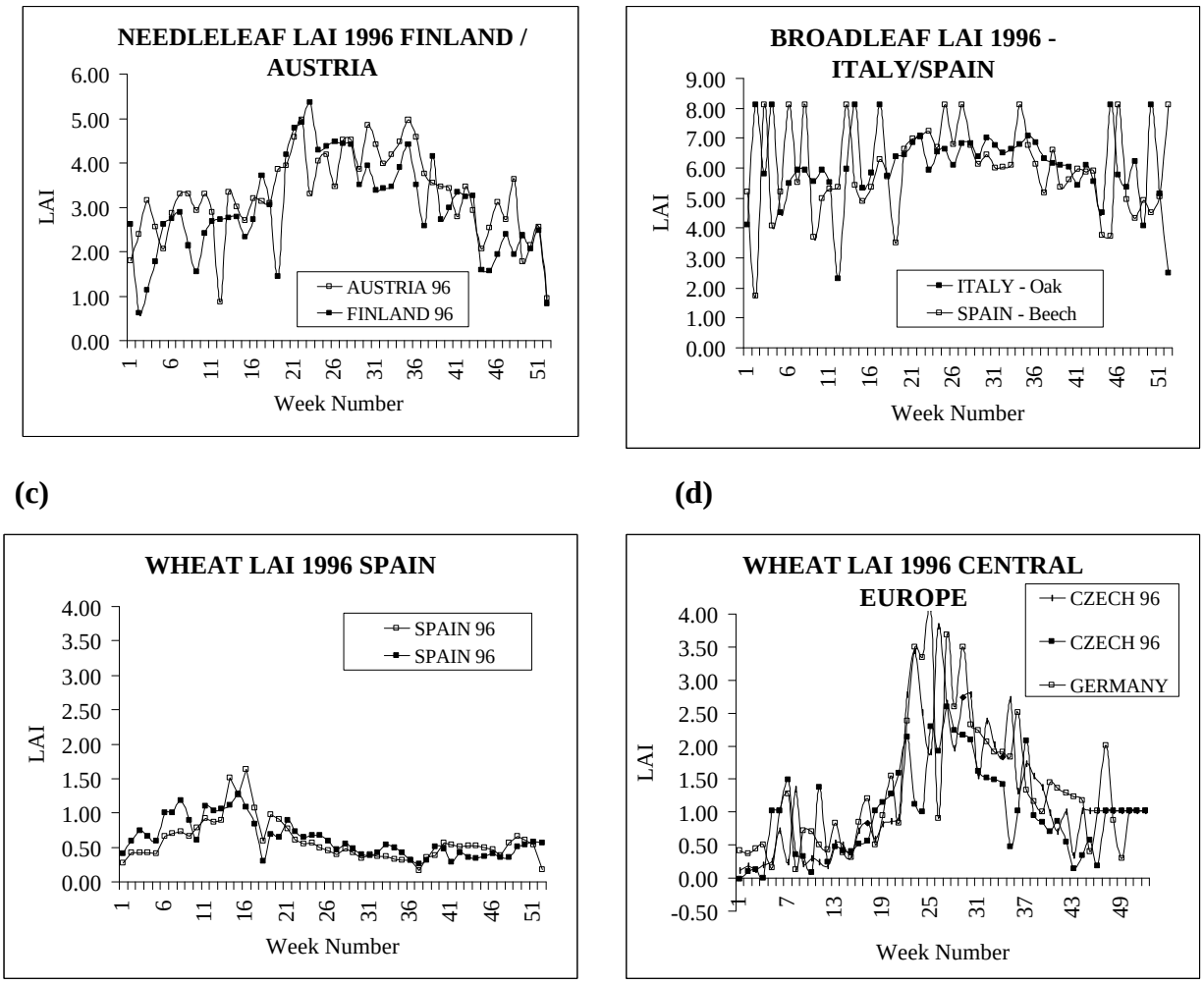

(c) **(d)**

In summary, whilst the calculated LAI does vary over the year, the profiles shown in Figure 3.9 and 3.10 do not follow the expected patterns of temporal variation when viewed either as weekly or monthly time intervals. This is clear from comparison with Figure 3.3 in the previous section, which describes the current model parameterisation based on literature values. The monthly profiles in Figure 3.9 and the weekly profiles in Figure 3.10 frequently fail to pick up major events strongly influencing LAI - such as bud-burst, senescence or leaf-fall. Considering these results alongside the raw NDVI data in Figure 3.8, it appears that although the satellite data may provide a valuable continental scale picture of LAI, it fails to represent the detailed land cover-specific variation that is required as inputs to the model.

The LAI calculation method employed by Sellers et al. (1994) sets constraints for the maximum attainable LAI - 5 for agricultural land, 8 for needleaves and 7.5 for broadleaves. Maximum LAI can however be higher for each of these cover types. Further investigation is required to assess the effect of setting different maximum LAI values. The difference between weekly and monthly LAI profiles is possibly due to the maximum value compositing technique used in the satellite processing routine to create the monthly dataset, which selects the highest NDVI value following the exclusion of cloud data and missing data. Whilst this smoothes out certain solar and atmospheric effects it may not be representative of the actual variation in LAI on the ground over the course of the month.

The key problem identified in this exercise is that the calculation of satellite derived LAI is sensitive to a variety of factors, including sensor saturation, viewing angle, scale considerations, mixed canopy reflectances and canopy illumination. Whilst a simple method of converting satellite NDVI data into LAI values could be applied within the ozone deposition modelling routines, there are a number of major reservations to incorporating it routinely. Firstly, satellite data have a number of inherent problems that affect secondary data outputs such as NDVI; these are related to sensor design and operation, atmospheric effects and global and solar movements. Secondly, both the satellite data and SEI land cover data should be available in exactly the same projection co-ordinate system or there should be sufficient parameterisation for the rectification of one data set into the other is required. Thirdly, the relationship between NDVI and LAI for some cover types during summer months is difficult to quantify as NDVI becomes saturated. Finally, the failure to detect individual land cover classes within an NDVI pixel reduces the overall effectiveness of the LAI algorithm. The uncertainties that have become apparent in this exercise lead to the conclusion that the use of satellite derived LAI for the purposes of modelling ozone uptake across Europe requires further validation before it can be routinely employed.

3.9 Soil Moisture Deficit

The second major problem for parameterisation is soil moisture deficit (SMD), which has a major influence on ozone flux and deposition, especially in southern Europe. Unlike the other terms, SMD is not available as a direct input, but needs to be calculated in a separate sub-model from climatic data; this calculation can be made species-specific and is also dependent on soil type. The results described in section 4 of this report do not include the effect of SMD on stomatal conductance and hence ozone deposition. This was for two reasons. Firstly, and perhaps most importantly, due to uncertainties in the NWP precipitation and surface air temperature data, parameters that are crucial for modelling SMD. The data that were available for 1996 at the 50 x 50 km scale were known to contain errors, however, by the time of publication of this report, these problems should largely be

overcome. Secondly, the SMD sub-model that had been developed had not previously been tested. Since the SMD model involves a number of assumptions that could affect final deposition results quite significantly, it was considered advisable to perform a preliminary test of the SMD model before its incorporation into the EMEP ozone deposition module.

In the latter stages of the research project, such a test of the model was undertaken, making use of data acquired for 3 sites in England during the early U.K. stage of the contract. Although this test by no means comprehensively determines the predictive capabilities of the SMD model, it represents an important advance towards assessing whether the SMD model, with some future improvements, may be suitable for use within ozone deposition and stomatal flux modelling. Full details of this work are provided in a project report in the Annexe.

The model test used three different methods to calculate SMD. The first was based on a method described by Mintz and Walker (1993) which calculates SMD according to the principles of a simple water budget model first developed by Thornthwaite in 1948. This method was recently incorporated into the EMEP photochemical model to provide indications of the effect of SMD on ozone deposition as described in Simpson et al. (in press), this paper is included in the Annexe to this report. The second method is that which will be considered for further development and implementation within the ozone deposition model and will here be referred to as the SEI-Y SMD model. This method is almost identical to the Mintz and Walker (1993) method with the following exceptions :-

1) The SEI-Y method derives land-cover specific root zone storage capacity (W*) values from vegetation group and species-specific root depths (Jackson et al. 1996) and permanent wilting point (PWP) values (Emberson, 1997).
2) Outside the assumed growing season, evapotranspiration (Et + Es) is set equal to 60% of that during the growing season.

Finally, the third method used to calculate SMD is the MORECS method that is used by the UK Meteorological Office. This method is more data intensive and involves estimating the canopy resistance as part of the model input; the method is based upon the Penman-Monteith formula, and has been extensively compared with field data in the U.K..

Initially all three models were compared for Marham, one of the 3 sites in the UK for which MORECS data were available, during 1994, assuming a medium soil texture type. These comparisons (Figure 3.11) showed that the MORECS and SEI-Y methods gave very similar estimates of the accumulation of SMD over the course of the year. By contrast, the Mintz and Walker (1993) method gave similar predictions of SMD up until around the end of June. After this time, the SMDs predicted by this model were greater and recharge was estimated to occur over a longer period of time, compared with the other two models. Figure 3.11 emphasises the importance of using the correct W* value and reducing Et+Es once the growing season has finished since it is these two variables that respectively produce the higher estimations of SMD and result in the slower recharge of the Mintz and Walker (1993) method.

Figure 3.11 Comparison of SMD calculated using Mintz & Walker (1993), SEI-Y and MORECS methods for the Marham site.

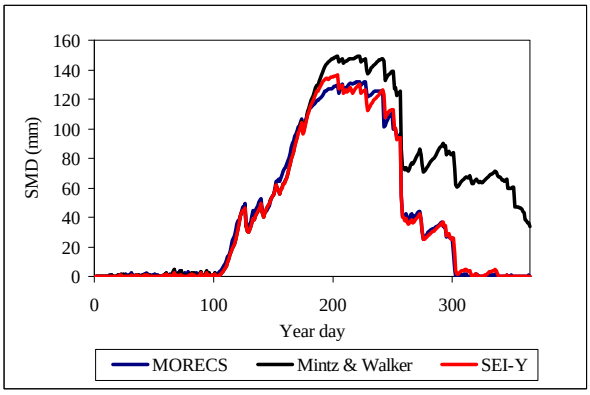

Further comparisons involving only the SEI-Y SMD and MORECS methods were made for all three UK sites and for all three soil textures. As a general rule, the SEI-Y model predictions of annual SMD are close to those predicted by MORECS. However, the SEI-Y model predicts MORECS SMD better for some soil types than other. This is predominantly due to differences in the value of W*, especially on coarse and fine soils, again emphasising the importance of this parameter.

To give an indication of the variability in the annual course of SMD between different land-cover types the SEI-Y model was also run for three other cover types : temperate coniferous, temperate deciduous and root crops. The results of this modelling are shown in Figure 3.12 for both 1994 and 1995. Figure 3.12 shows the SMD calculation for medium soil textures. The two crop types produce very similar annual soil SMD profiles. However, the SMD under temperate coniferous and temperate deciduous trees is much greater, as a result of the longer growing seasons assumed for these species types. Temperate deciduous trees are assumed to grow from year day 90 to 270 whilst coniferous temperate species are assigned a year long growing season. In the case of temperate coniferous species, the deeper roots will make available a larger reservoir of soil water allowing more soil water to be lost from the system when the potential for evapotranspiration is high.

Figure 3.12 SMD for medium soil type for four land-cover types for Marham during 1994 and 1995.

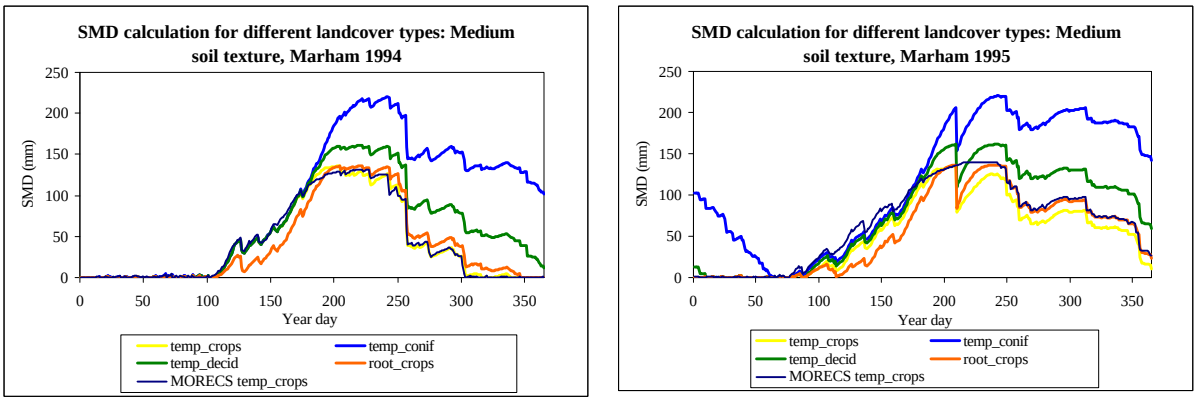

Figure 3.13 shows the modelled influence of SMD on stomatal conductance for each land-cover type (g_{SWP}). These graphs only show a proportion of the year (from day 150 to 300)

and hence it is apparent that the limiting influence of SMD on g_{SWP} tends to be confined to the summer months. The early end to the growing season for temperate crops means that they largely "avoid" the period with the highest SMDs. It is also worth noting that the brief period during which SMD is modelled to reduce g_s for these temperate cereals occurs just before harvesting during what is now widely recognised as the most ozone sensitive phenological period for wheat (e.g. Pleijel et al., 1996). The g_{SWP} profiles for temperate deciduous and root crops are similar with the exception that in 1995 the soil water content of the root crops does not recharge before harvesting. These two vegetation groups are modelled to be those most affected by SMD in terms of reductions in stomatal conductance. Finally, temperate conifers only experience a short and relatively small limitation to stomatal conductance. This emphasises the importance of the rooting depth since although the coniferous species were modelled as inducing the largest SMD, the maximum root depth of 1.23 m means that this species has access to a large reserve of water. Therefore, the potential for evapotranspiration has not been sufficiently high to have depleted these reserves. As such, the soil only reaches its maximum SMD on a few occasions during the year and consequently g_s is relatively unaffected.

Figure 3.13 g_{SWP} for medium soil types for four land-cover types for Marham during 1994 and 1995.

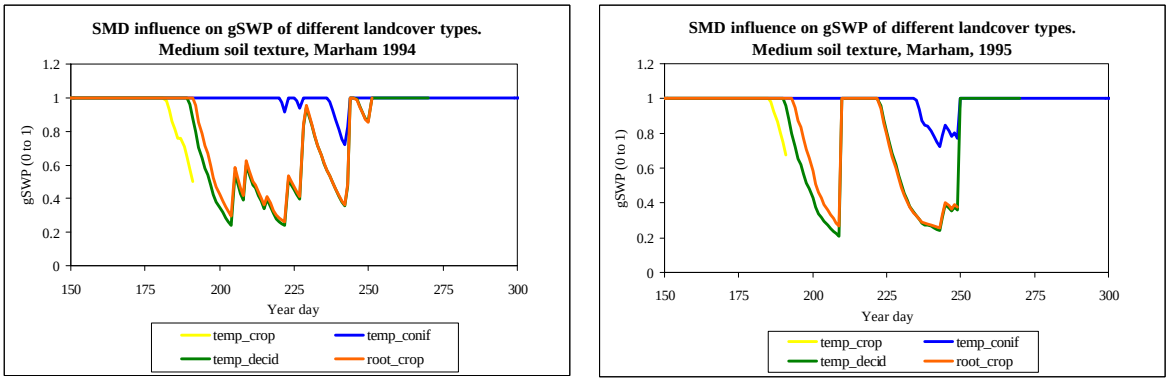

The difficulties in assigning values for rooting depths represents one of the main uncertainties in the SEI-Y SMD method. Figure 3.14 shows the effect on SMD accumulation and subsequently on g_{SWP} of varying root depths (0.8, 1, 1.2 and 1.4 m) for the temperate conifers and deciduous vegetation groups at the Marham site during 1994. The effect on g_{SWP} is quite dramatic. At low rooting depths stomatal conductance is often reduced, but as the roots grow deeper, influence of SMD on g_s is lessened. For the deepest root depth (1.4 m) this actually results in no modelled influence on g_{SWP}. The deciduous and temperate vegetation types have very similar annual profiles as would be expected when using the same root depth inputs. The differences that do exist are a result of the g_{SWP} parameterisation, especially for SWP_max (–0.55 and –0.76 MPa for deciduous and coniferous species respectively). This difference results in the deciduous species experiencing longer periods of lower g_s and highlights the importance of the specific g_{SWP} parameters in addition to using appropriate root depths within the model.

The issue of selecting appropriate rooting depths for vegetation needs further investigation, especially given the differences in root depths of species within vegetation groups that are likely to exist. Root depth values within the SEI-Y model are based on data given by Jackson et al. (1996) where the root depth represents the depth within which 95% of the root biomass exists. It would be interesting to perform future SMD model runs using maximum rooting depths (as compiled by Canadell et al. 1996), which may be more

biologically meaningful in that the plant may be expected to increase root growth under times of drought stress. However, some plant species are known to use hormonal signals from the roots to the aerial plant parts which lead to stomatal closure under drought conditions (e.g. Davies et al., 1994); this may result in stomatal reduction to g_{min} before the SMD has reached the vegetation specific PWP.

Figure 3.14 The effect on SMD accumulation and subsequently on g_{SWP} of varying root depths (0.8, 1, 1.2 and 1.4 m) for temperate conifers and deciduous vegetation groups at the Marham site during 1994

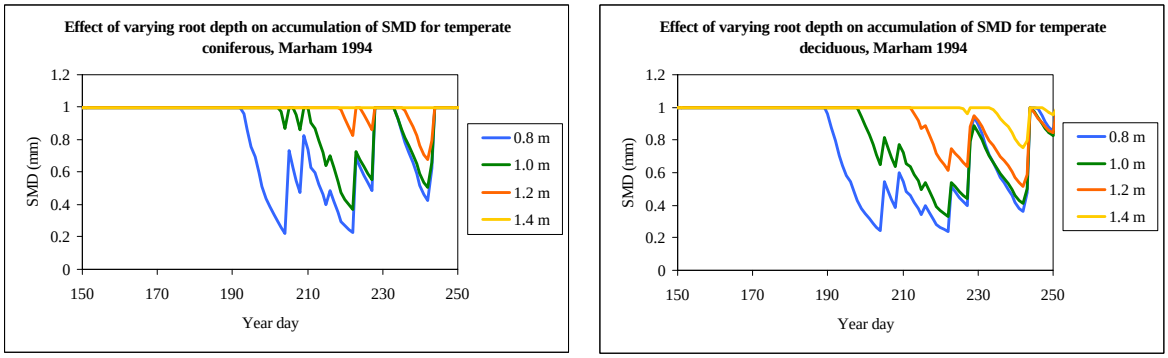

The model results presented here can also be compared with those presented by Simpson et al. (in press) as part of a wider sensitivity analysis of the EMEP deposition model (see 5.4 below. Mean monthly profiles (May and June) of deposition velocity (Vg) were modelled for four sites across Europe (Finland, Scotland, Switzerland and Portugal) for both temperate coniferous and crop vegetation types. It was found that SMD only influenced Vg for the Portuguese site and only for the forest vegetation type. This is consistent in terms of the results of this exercise in the U.K., in that during May and June no influence of SMD on g_{SWP} was found. Most importantly, Simpson et al. (in press) show that the influence of SMD on g_{SWP} translates into a significant reduction in Vg. Accurate modelling of this phenomenon will be crucial especially in the hotter climatic regions of Europe.

4. RESULTS

In this section, we show the results of model simulations and summarise the main features of the model runs. A more detailed assessment of the results of these simulations in the context of existing knowledge of deposition processes is provided in Section 5.

Calculations have been performed for several locations in Europe, using meteorological data from the EMEP 50 x 50 km^2 data sets, with 3-hourly resolution. As noted earlier, all results are calculated for the well-watered situation, i.e. assuming $g_{SWP}=1$. The example sites were chosen so as to represent different climatological conditions. These grid squares are named according to specific sites located within the square at which field measurements of ozone fluxes have been performed, to assist in the comparisons described in Section 5. The sites are: -

Petsikko, Finland (latitude 69^oN)
Auchencorth Moss, Scotland (latitude 56^oN)
Payerne, Switzerland (latitude 47^oN)
Montemor, Portugal (latitude 39^oN)

At each site the calculations were carried out for each land-cover type included in the model that employs the parameterisation of the stomatal conductance. This means that, except for a few cases, the data do not refer to actual ecosystems. We discuss here some initial observations on the model results, including both stomatal and non-stomatal pathways.

Figures 4.1 and 4.2. illustrate the calculated values of deposition velocity, canopy stomatal conductance, and g-factors for six land-cover types for the Scottish location. It is important to note that the months used for some parameters differ between land cover types. These figures allow comparison of the modelled results for the different land cover types. In terms of deposition velocity, the expected seasonal variation is found, with low values in winter and the highest values in summer. The highest summer deposition velocities are for forests, root crops and grassland; by comparison, temperate crops and moorland. The values of canopy conductance similarly show a strong seasonal variation, as well as a strong diurnal variation that influences the deposition velocity. The maximum canopy conductance shows a different pattern with land-cover. The highest values are for grasslands and root crops, with the values for forests being comparable to those for moorlands and temperate crops. Hence, the high deposition velocities for root crops and grasslands at this location are due to the high values of canopy conductance, while those for forests are more to the low aerodynamic resistance.

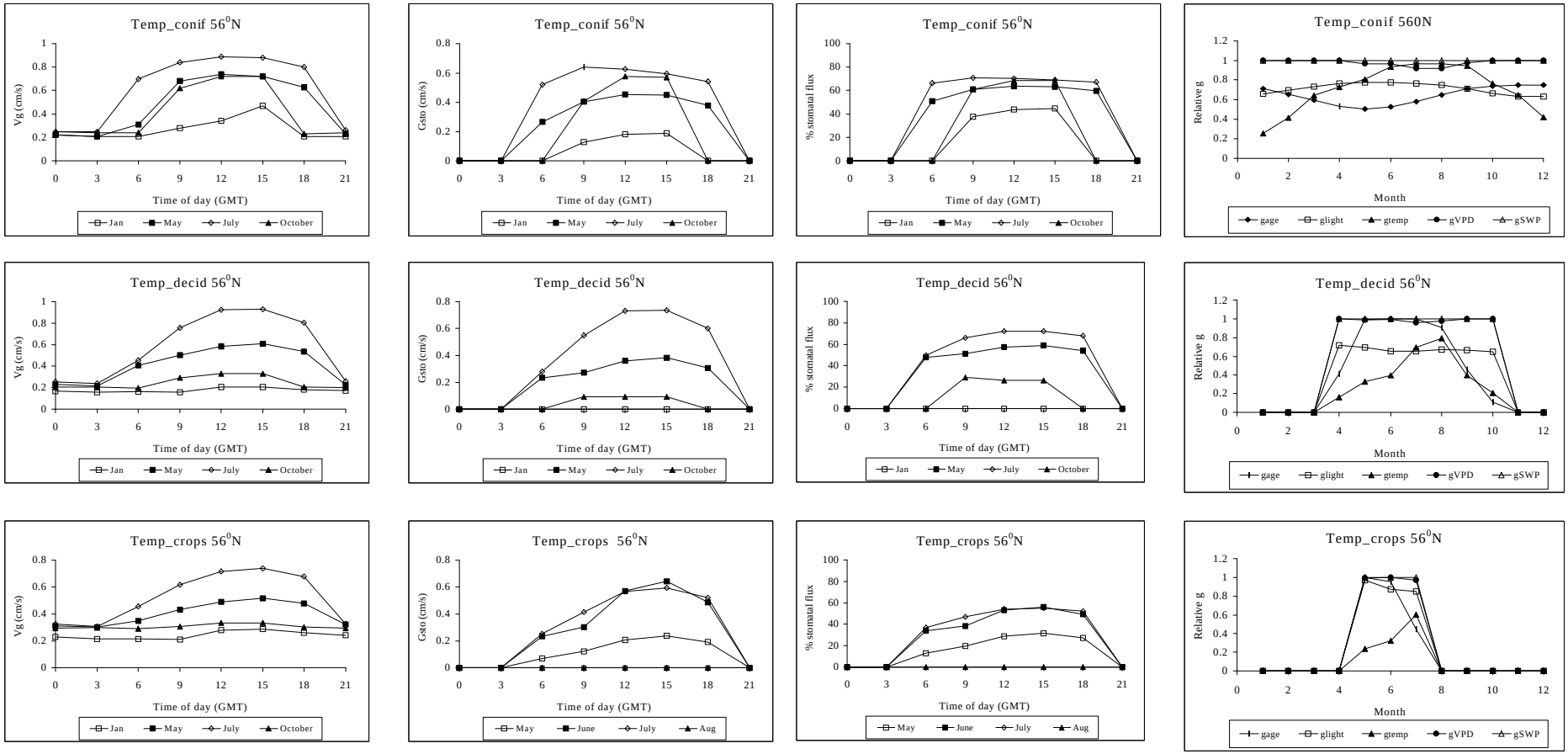

Figure 4.1 **Calculations for Auchencorth Moss, Scotland. From left to right: (a) near surface deposition velocities (Vg) (1/(Ra(d+3m)+Rb+Rsur)), (b)canopy stomatal conductance (G_{sto}), (c) % of canopy stomatal component of surface deposition, (d) noon-time g-factors. Results given as monthly averages, calculated when LAI > 0 for 5 days or more during a month.**

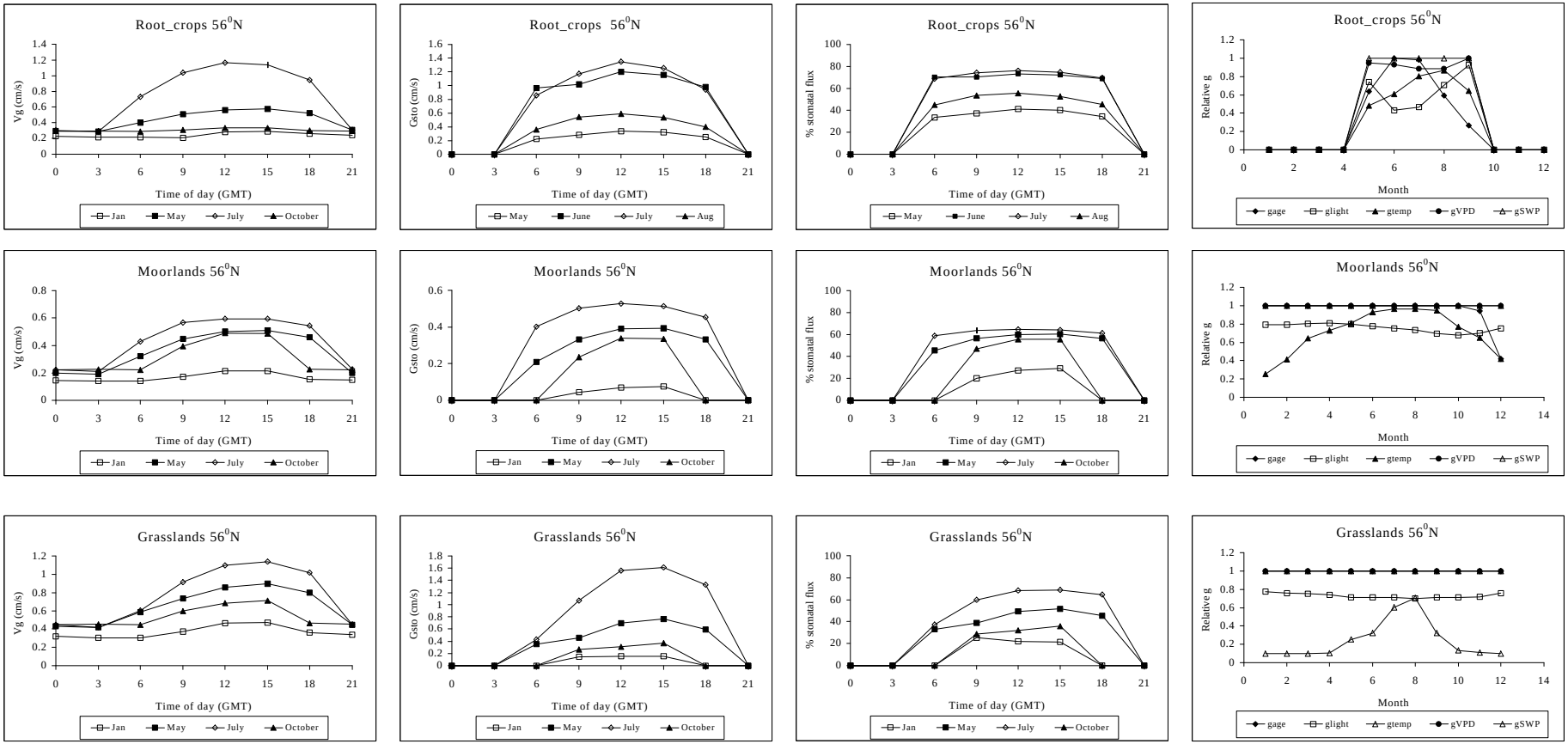

Figure 4.2 **Calculations for Auchencorth Moss, Scotland. From left to right: (a) near surface deposition velocities (Vg) (1/(Ra(d+3m)+Rb+Rsur)), (b)canopy stomatal conductance (G_{sto}), (c) % of canopy stomatal component of surface deposition, (d) noon-time g-factors. Results given as monthly averages, calculated when LAI > 0 for 5 days or more during a month.**

The calculated values of the proportion of surface deposition that is attributable to stomatal uptake are of considerable interest. At midday in the summer, this value is 60-80% of all deposition for most land covers, although the values for grasslands and temperate crops are somewhat lower. These high contributions of the stomatal term correspond to periods of high absolute deposition rate. However, if these modelled values are integrated over the whole year, then the contribution of stomatal deposition varies between 25% and 50% for the different land covers. The lowest value is for temperate crops; however, if the percentage of stomatal deposition over the year at the four different sites is compared for forests and cereals (Table 4.1), then the value is particularly low at this site. The range of values for all sites is no greater than that at the Scottish site, but a clear conclusion is that, while stomatal uptake dominates periods of peak deposition, in terms of total annual deposition, the non-stomatal pathway is at least as important, if not more important, under the assumptions of our model.

The final column of Figures 4.1 and 4.2 show the variation in the limitation to stomatal conductance from different factors (excluding soil moisture deficit). It is important to note that these are calculated as an average over each month, and the limitation may be considerably higher at specific times of high ozone concentration. For most of the land-cover types, temperature causes the greatest limitation to stomatal deposition over the year; there is also an effect of light and of age/phenology.

Table 4.1 Percentage of annual total deposition due to stomatal uptake at four sites for forests and cereals

Location	**Forests**	**Cereals**
Finland	44%	40%
Scotland	49%	26%
Switzerland	51%	41%
Portugal	39%	40%

Having considered the broad features of the model predictions for different land covers at the same location, it is of interest to compare the differences between location. For simplicity, these differences are presented for one land-cover type – coniferous forests – chosen because of the relatively high deposition velocities and because vegetation is present all year. We emphasise in describing these variations between location that the same parameterisation has been used across Europe; in practice, differences in LAI, SMD and stomatal functions would be expected.

Figure 4.3 shows the monthly mean deposition velocities for the four locations, together with the importance of the different component resistiances. At all locations, the aerodynamic and boundary layer resistances were small compared with the canopy resistance, although they might be expected to be more significant for shorter vegetation. Simulations for temperate cereals, for example, suggest that their overall contribution could approach 50%. The seasonal patterns in Scotland and Switzerland are comparable, rising steadily to a maximum of about 0.55 cm s^{-1} in July/August, and then declining

steadily again. Deposition velocities are lower at the Finnish site, and there is a stronger seasonal variation. The seasonal pattern in Portugal shows two maxima, in the spring and autumn, with maximum deposition velocities that are intermediate between those in Finland and at the two other sites.

Figure 4.3 Monthly mean deposition velocities for temperate coniferous forests, together with relative importance of resistance components, defined as $F(R_x)$ from Simpson et al. (in press).

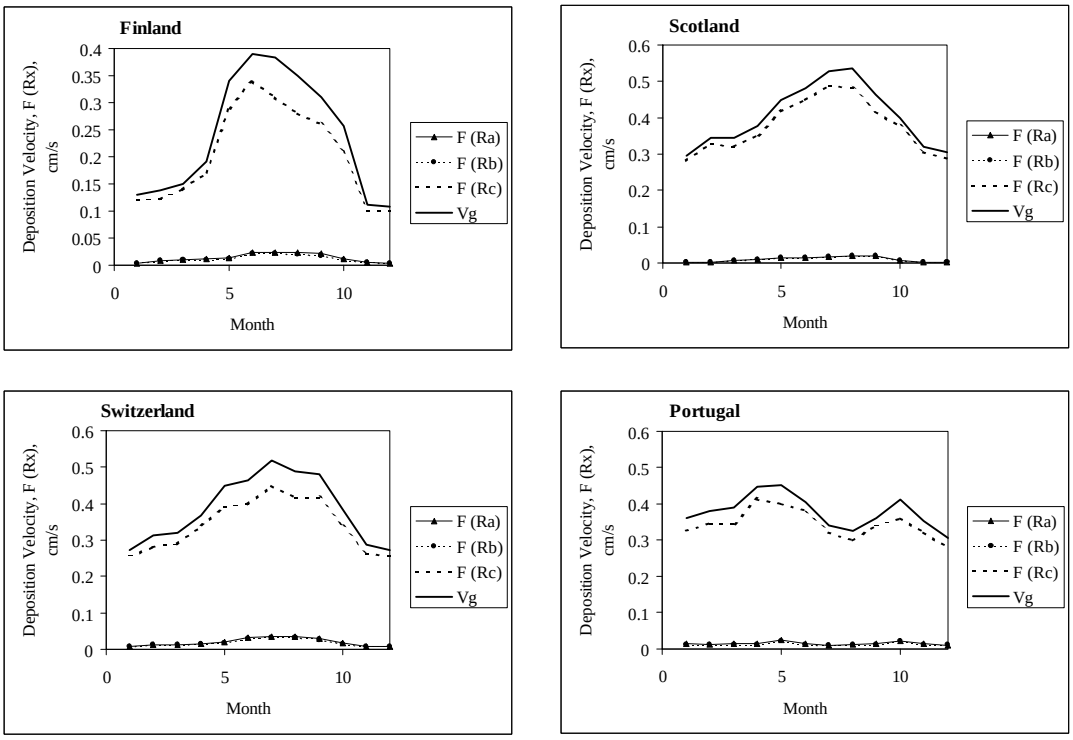

Figure 4.4 shows the diurnal pattern of deposition velocity for four months for temperate coniferous forests (note that these are not the same months at all locations). The variation between sites and months in night-time values is small, with the differences therefore primarily due to the variations in canopy conductance during the daytime.

Figure 4.4 Diurnal variation (times in GMT) in deposition velocity (Vg (z =50m)) for temperate coniferous forests. Calculations are monthly averages, and taken at 3-monthly intervals from the month of the greatest Vg.

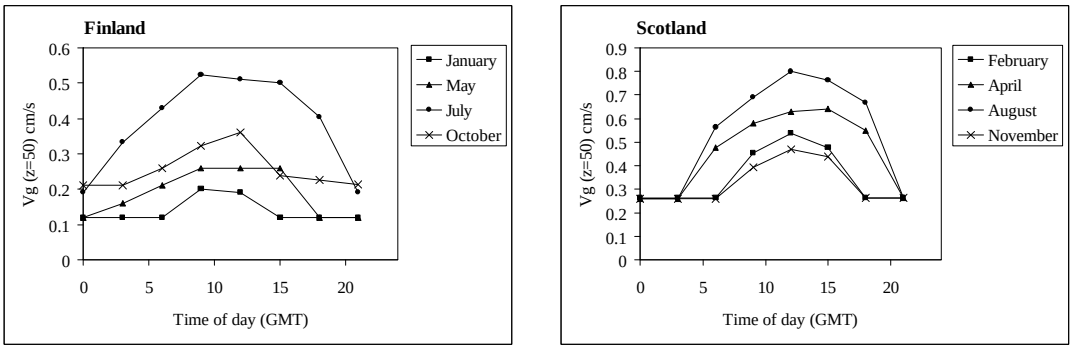

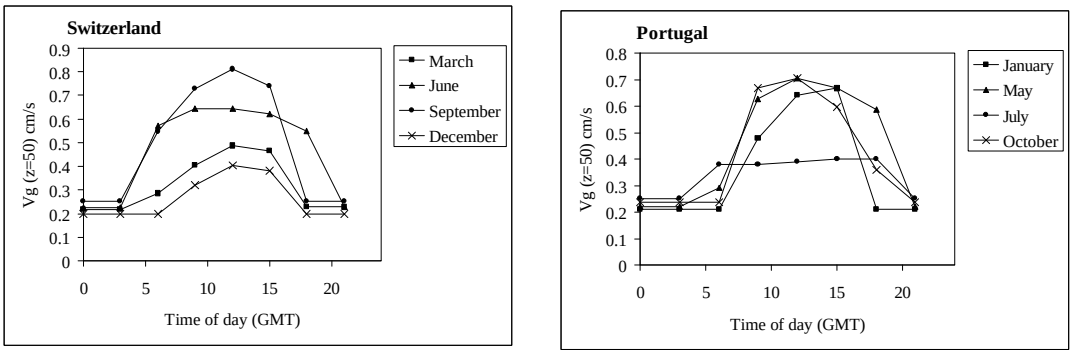

The variations in stomatal conductance that control these variations in surface resistance are illustrated in Figure 4.5., which shows the monthly variation in noontime stomatal conductance factors. There is a clear contrast between the Portuguese location and the other three. In Switzerland and Scotland, the lower values in the winter are due primarily to temperature limitations; this is a stronger factor at the Finnish site, where there is also a much stronger effect of light limitation. Vapour pressure deficit has no effect in Finland and Scotland, although its effect on individual days of high ozone concentration could be greater; this parameter has a small effect in Switzerland in summer, and a strong effect in the summer at the Portuguese site. Temperature does not limit stomatal conductance at the Portuguese site in winter, but does have an effect in summer. There is also a strong effect of soil moisture deficit at the Portuguese site in late summer, which is not apparent at the other sites.

Figure 4.5 Monthly variation in noontime stomatal conductance factors for temperate coniferous forests

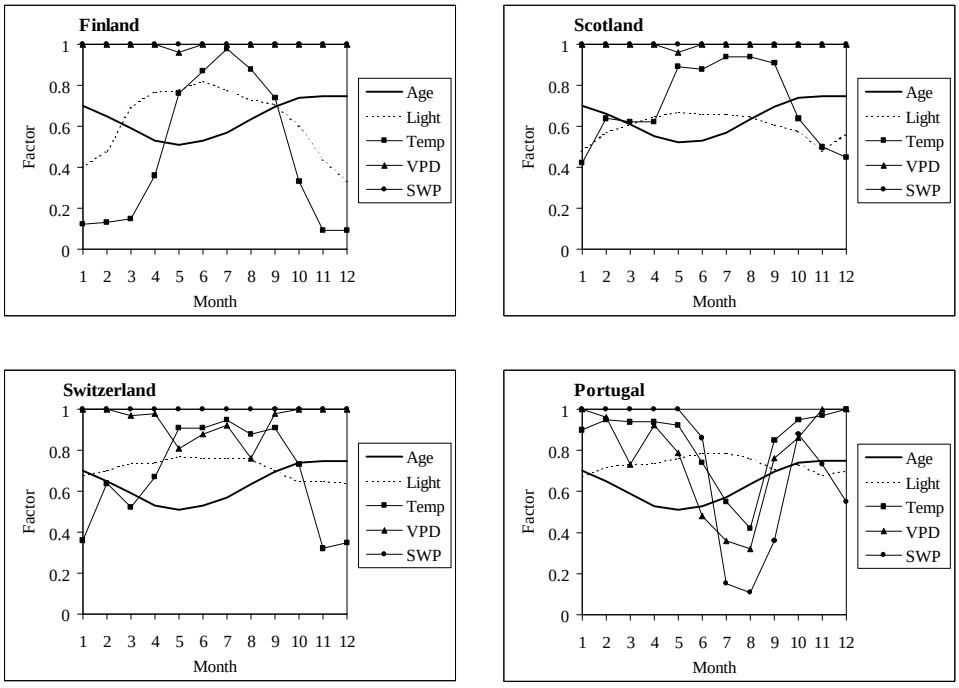

5. MODEL EVALUATION

5.1 Introduction

A key element of the research conducted under this contract has been to critically evaluate the performance of the model. This assessment of the performance of the model has involved three major elements:-

a). Direct comparison with primary field and experimental data, either of stomatal conductance or of deposition, or deposition components. This has involved direct comparisons of model predictions using the parameterisation described above, or has involved a modified version of the model parameterised for local site conditions, because of the importance of distinguishing systematic errors in the model formulation and assumptions from errors due to inappropriate parameterisation.

b). Broad comparison of predicted deposition rates with published field measurements of deposition rate. This has involved comparison of the model simulations described in Section 4 above with the range of values reported for a particular land-cover. Hence these comparisons are not site-specific. However, the comparisons of model outputs with published data are made as far as possible with those results that closely match the time of year, time of day, prevailing climate, land-cover type and geographical location. These comparisons give a general idea of the model's capability to predict values within the range of published data.

c). A sensitivity analysis, to assess which parameters and/or assumptions have the greatest influence on the deposition velocities predicted by the model. This analysis contributes to the identification of critical aspects of the model which require further development or improved parameterisation.

The following sections summarise the results of each of these aspects of model assessment in turn. As before, further details can be found in the documentation included in the Annexe to this report. It is also important to realise that assessment of the validity of model input parameters and data, such as the method used to estimate soil water deficit, or to scale from leaf to canopy, are also important elements of model assessment. These were discussed in detail in Section 3.

5.2 Primary field and experimental data

(i) Scots pine deposition; Finland

The first comparison with field data was performed by Tuovinen (2000) for a Scots pine forest in Finland (63°N). The results calculated by using the default land-cover specific values of canopy height and leaf area index were unsatisfactory. The mean midday maximum of the surface conductance measured in July 1995 was 0.67 cm s^{-1}, which is about 50% of the model prediction. For a sparse forest, such as this, with a LAI of about 2, the default values are not representative and are expected to lead to overestimated deposition rates and surface conductances.

However, when tested in a site-specific mode, adjusting the canopy parameters according to local conditions and also using *in situ* meteorological observations, a satisfactory fit with observations was obtained, as shown by the mean positive bias of 16% in the deposition velocity (Tuovinen, 2000). The results of this comparison are shown in Figure 5.1, in

which where observed and modelled surface conductance values are shown. The modelled G_{sur} (in m s^{-1}) values are also similar to the observed values when the local input data and LAI value is used in place of the EMEP meteorological data and default LAI parameterisation.

Figure 5.1 Surface conductance to ozone for a sparse Scots pine forest growing in Finland. Comparisons are made between observed and modelled data using local vegetation parameters and meteorological input.

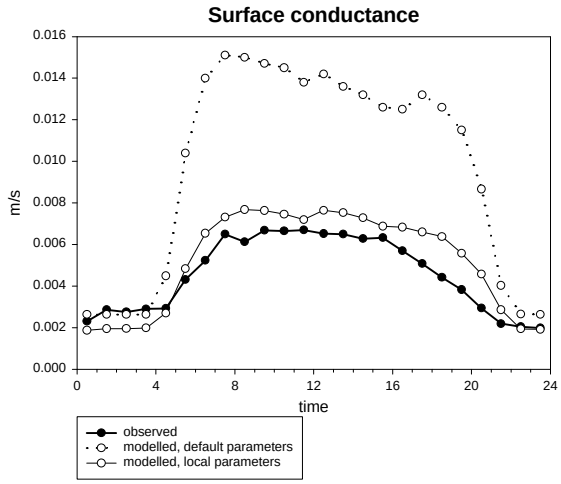

The slight tendency for the model to over-predict the deposition rate was not found at the highest rates, which were under-predicted. The residual between the observed and modelled surface conductance did not depend on air temperature, PAR or VPD. However, the under-prediction of G_{sur} coincided with the highest friction velocities, which may be related to the simple parameterisation of the aerodynamic in-canopy resistance. Overall, this example demonstrates that the model is capable of predicting the mean summertime deposition velocities, but also that considerable uncertainties result from aggregating forests with a wide density range into a single land-cover category.

Because of the role of LAI in the parameterisation, a corresponding under-prediction could be expected at sites with a LAI larger than the default value. For coniferous forests, this should be true for spruce stands. Pilegaard et al. (1995a) measured a mean daytime surface resistance of 150 s m^{-1} (G_{sur}= 0.7 cm s^{-1}) for a 12-m Norway spruce plantation in Denmark in June 1994 and a much higher value of 370 s m^{-1} (G_{sur}= 0.3 cm s^{-1}) for the dry month of July 1992. These correspond to a considerably lower surface conductance than predicted by the model. The reason for the differences is not clear. On the other hand, the measurements during a winter month show a mean daytime surface resistance of 210 s m^{-1} (Pilegaard et al., 1995a), which is close to the model predictions.

(ii) Norway spruce stomatal conductance; Austria

The second study compared measured and modelled stomatal conductance to ozone using site-specific meteorological and ozone data for a montane site in Austria with the core stomatal conductance model Norway spruce parameterisation (Emberson et al. 2000b). The model performed reasonably well, accounting for 66 % of the variation in stomatal conductance to ozone (GO_3) to individual needles. In addition, the model was capable of describing monthly mean diurnal variation in stomatal conductance with reasonable

accuracy (e.g. Figure 5.2). However, this study also highlighted the importance of assigning the correct g_{max} value, since the use of a value consistent with local conditions improved the predictive capabilities of the model.

Figure 5.2 Comparison of modelled and measured average diurnal values of GO_3 for Norway spruce (*Picea abies*) during the 1989[(a)] investigation period (Emberson et al. 2000b). The measured and modelled values are represented by filled and open squares respectively.

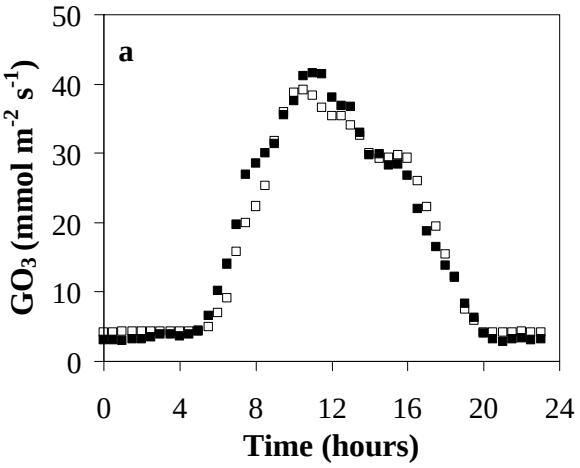

(iii). Norway spruce stomatal conductance; Sweden

A further comparison of modelled and measured values of stomatal conductance was made for young Norway spruce trees in an open-top chamber experiment in Sweden by Karlsson et al. (2000). This experiment involved a comparison of droughted and well-watered seedlings. As for the field comparisons for this species, a good correlation between measured and predicted values was found when the default parameterisation was replaced by local parameterisation for the experimental material. However, two physiological effects were observed which had not been included in the core stomatal model. Firstly, it appeared that drought treatment in one year reduced g_s in the subsequent year through some sort of 'memory' effect. Secondly, the droughted seedlings were more responsive to vapour pressure deficit than the well-water seedlings, implying an interaction between the two environmental factors. The significance of these two observations for model performance under field conditions requires further investigation.

(iv). Cumulative ozone dose in beech; Germany

The final use application of the model to field data was not strictly speaking a validation or assessment exercise, but the results are of considerable interest. The application was to mature beech stands in southern Germany, in which the first appearance of visible leaf injury was recorded at different sites and in different years. The cumulative seasonal AOT40 exposure before injury first appeared had been calculated, and the interest was to assess if the use of the model to estimate cumulative stomatal uptake provided a different estimate of the threshold for visible injury.

A key feature of the results was the remarkable consistency of the threshold values of modelled cumulative ozone uptake. The cumulative stomatal uptake before the onset of

visible injury on mature trees in the field was 3.0-3.1 mmol O_3 m^{-2} for two sites in both 1995 and 1997, and also in phytotron experiments with seedlings using ambient ozone exposure regimes. In contrast, the cumulative threshold value of AOT40 varied by an order of magnitude, from 500 ppb.h to 6000 ppb.h across the sites and years. Although this is circumstantial evidence, rather than a direct test of the mode, it does indicate that, despite the greater body of data needed to estimate stomatal uptake, the model can provide predictions which are much more closely related to observed effects than are AOT40 values.

5.3. Published data on deposition velocities

Table 5.1a compares published values of ozone deposition velocities (collated by Brook et al. (1999)) and Table 5.1b compares canopy conductance (collated within this project) with comparable model results (shaded columns). The summary below briefly assesses the model performance in these various comparisons; further details are given in the EMEP note in the Annexe.

For coniferous temperate species, the values compiled by Brook et al. (1999) suggest that the mean and maximum modelled deposition velocities (cm s^{-1}) underestimate actual values. This could well be a result of the default maximum LAI value of 4.5 m^2/m^2 being too low for mature pine and spruce forests. When the model was applied to field measurements with a recorded LAI effect. e.g. a Sitka spruce stand where LAI reaches approximately 10 m^2/m^2 (Coe et al. 1995), a better agreement was found (Table 5.1b). In general, when differences in LAI are taken into account the modelled values are in good agreement with field observations, with the phenological component being well described (e.g. Slovik et al. 1996) as well as the effect of VPD in decreasing afternoon canopy conductance (Sturm et al. 1998). The model was also found to be capable of predicting the small but significant night-time deposition observed by Pilegaard et al. (1995) and Tuovinen et al. (1999). The model also predicts the reduced surface conductance during winter that results from the deposition to external non-stomatal surfaces.

Table 5.1 Comparison of measured values with modelled estimates for a) total ozone deposition velocity and b) canopy stomatal conductance. All values are given as ozone conductances in units of cm s^{-1}.

a) Deposition velocity comparisons

Surface	Observation				Modelled		
	Mean	Range	Condition	Reference	Land-cover type	Mean	Range
Beech	0.4	0.1 – 0.7	April, May	Pilegaard et al (1995b)	DF	0.41	0.22 – 0.78
Deciduous forest	1.0	0.0 – 1.8	Dry day summer	Padro et al. (1992, 1994)	DF	0.5	0.25 – 0.82
		0.0 – 1.2	Wet day summer				
	0.2	0.0 – 1.2	Night summer			0.24	
		0.0 – 0.5	Dry winter			0.18	0.12 – 0.25
		0.0 – 0.4	Wet winter				
		0.11 – 0.45	Winter	Wesely et al. (1983)		0.18	0.12 – 0.25
		0.23-0.45	Day winter				0.15 – 0.23
Grape		0.02 – 0.92	No dew	Massman et al. (1994)	V	0.7	0.1 to 1.3
		0.01 – 1.02	Dew				
Grass		0.05 – 0.2	Summer	Padro (1996)	GR	0.58	0.3 – 0.89
	0.56	0.06 – 1.0	Daytime	Delany & Davies (1983)		0.67	0.58 – 0.89
		0.0 – 0.56	No dew	Massman et al. (1994)			
	0.24		Summer	Meyers et al. (1998)		0.58	
Pine forest		0.0 – 1.16		Sanchez & Rodriguez (1997)	CF	0.39	0.18 – 0.73
	1.0		Summer	Lenschow et al. (1982)		0.48	0.22 – 0.74
Spruce		0.0 – 0.7	June	Pilegaard et al. (1995a)	CF	0.51	0.22 – 0.74

b) Canopy stomatal conductance comparisons

Surface	Observation	Condition	Experimental apparatus, Location	LAI	Calculation	Reference	Land-cover type	Mean	Range
Scots pine (*Pinus sylvestris*)	May: 0.6 June: 2.4	Daytime	England	7.5 – 11.3	Calculated from g_s and LAI allowing for height within the canopy and needle age	Roberts et al. (1982)	CF	May: 0.38 June: 0.49	
Sitka spruce (*Picea sitchemsis*)	Max: 0.5 Range: 0.016 – 0.5 (Daytime)	Diurnal	Field, Scotland	10.2	Calculated using eddy correlation techniques with Penman Monteith equation	Coe et al (1995)	CF	Max: 0.45	0.26 – 0.45 (daytime)
35 yr. Old Scots pine (*Pinus sylvestris*)	Max: 0.31 Range: 0.0 – 0.31	June, Diurnal	Field, Germany	3	Calculated from sapflow	Sturm et al. (1998)		Max: 0.58 Mean: 0.33	Range: 0.0 – 0.58 (diurnal)
40 – 140 yr old Norway spruce (*Picea abies*)	Max: 0.24 (10.00 Hrs) Mean: 0.15 (Daytime) Range: 0.01 – 0.24	Diurnal	Field, Germany	6.5	Calculated from sapflow	Köstner et al. (1998)	CF	Max: 0.61 Mean: 0.5 (Daytime)	0.0 – 0.61
35 yr old Beech (*Fagus sylvatica*)	Mean: 0.3 Range: 0.015 - 0.66	Daytime, June to September	Field, Italy	3.8	Calculated using Penman-Monteith equation.	Magnani et al. (1998)	DF	Mean: 0.23	0.0 – 0.86
32 yr old Sessile oak (*Quercus Petraea*)	Max: 2.5	Summer	Field, France	6	Calculated using Penman-Monteith equation.	Breda et al. (1993a)	DF	Mean: 0.23	0.0 – 0.86

Note that the references listed in this table are given in the Annexe of the EMEP note (Emberson et al., 2000c).

Comparing the modelled and observed deposition velocities compiled by Brook et al. 1999 for deciduous forest, the model also tends to underestimate deposition velocities. Maximum deposition velocities are recorded in Table 5.1a to be on average 0.5 and 1.2 cm s^{-1} in winter and summer respectively; in contrast the model predicts equivalent values of 0.25 and 0.8 cm s^{-1}. These differences are again assumed to be largely related to the use of the low default LAI value of 5 m^2/m^2.

More detailed comparisons with European field data give contrasting accounts of the change in deposition velocity to canopies with and without foliage. Higher deposition velocities measured in bare forest canopies have been attributed to the influence of the underlying forest vegetation, which could constitute an important sink for ozone outside the deciduous trees growing season and should be taken into account when modelling for this cover-type (Pilegaard et al. 1995b, 1997). The diurnal profiles of canopy conductance were found to be predicted reasonably well for warmer climates, where the higher afternoon VPDs are shown to result in stomatal closure and reduced canopy conductance (Magnani et al. 1988).

Very few measurement data exist for either of the Mediterranean forest types and those that do are inappropriate for comparison of deposition velocities due to the difference in LAI between the measurement site and the model default value. It is important to consider the importance of SMD in determining ozone deposition to these Mediterranean cover types. Figure 5.3 shows standardised published seasonal profiles of gmax for Holm oak (*Quercus ilex*), which is grouped within the Mediterranean broadleaf cover type.

Figure 5.3 Seasonal course of standardised midday g_s for *Quercus ilex* in different European locations. The Caldwell et al. (1986) data describes the course of g_{age} over the year i.e. that when no environmental limitation to g_s is being experienced.

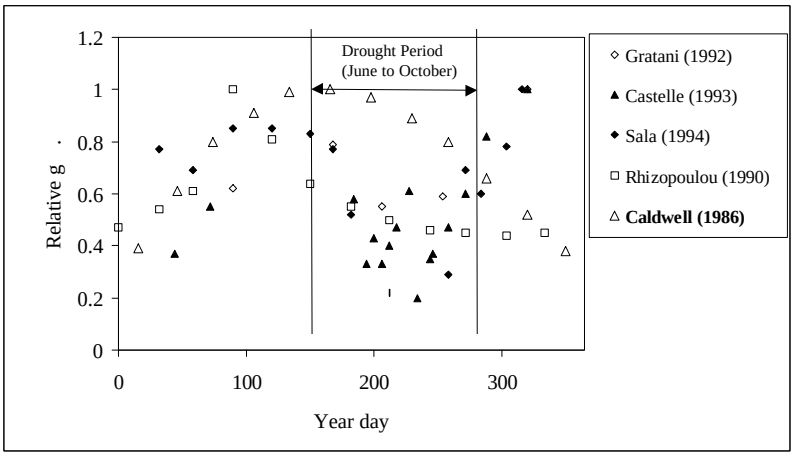

Figure 5.3 shows that g_s is significantly reduced between the months of June to October. This coincides with periods of drought and therefore, reflects the influence that reduced soil moisture availability will be likely to have on g_s, canopy conductance and subsequently ozone deposition.

For both crop types, few data describing deposition velocities exist. Deposition velocities measured in OTCs compare favourable with those predicted by the model at a similar climatic location (Grimm & Fuhrer 1992), while deposition velocities to wheat and to sugar beet recently measured in the U.K. are comparable to those predicted by the model.. Measured deposition velocities to a maize field in the Netherlands compare favourably with model predictions under a similar climatic regime (van Pul & Jacobs 1994).

The moorland category was modelled using a different approach from the other land-cover classes. There were insufficient literature data to parameterise the stomatal conductance model for this cover type. However, the availability of an exceptionally long-term flux measurement data set of four years available for an ombrotrophic mire in Scotland (Fowler et al. 1999) enabled the parameterisation of maximum g_s and non-stomatal conductance based on observations. The use of this parameterisation resulted in favourable model predictions of mean diurnal and annual cycles of deposition velocity for this cover type.

For grasslands, the model predicts relatively high surface conductance values and thus deposition velocities. With the exception of southern Europe locations, the model runs do not indicate a strong limitation to deposition by VPD. However, observations made in Germany (Grünhage et al. 1994) show a clearly asymmetric cycle that was attributed to VPD influences on stomatal conductance. In addition, the model seems to overestimate deposition velocity values compared to the German data although these long-term data warrant a site-specific comparison to properly test the model. Comparisons of model predictions with Mediterranean grassland types showed that the model was able to predict the seasonal stomatal component of deposition reasonably well when soil moisture was not limiting (Cieslik & Labatut, 1997) as well as total dry deposition during a five day period in late July (de Miguel & Bilbao, 1999). Further assessment is needed for periods when soil moisture deficit is limiting.

5.4 Sensitivity analysis

In the final phase, an analysis of the effects of variation in a range of input parameters was carried out. This analysis has subsequently been submitted for inclusion in a special issue of Water, Air and Soil Pollution; this paper (Simpson et al., in press) is included in the Annexe. This was not designed as a complete and formal sensitivity analysis, but rather examined the effects of different parameters and model assumptions in isolation. In cases for which a single parameter operated in a variety of ways (e.g. temperature has a direct effect on g_s and an indirect effect through changes in vapour pressure deficit), each process was examined separately. The predicted parameter examined was the mean deposition velocity over a three-month growing season for crops and a six-month growing season for forests. It is important to note that the sensitivity analysis might have had different conclusions if other parameters had been examined. The main conclusions of the analysis were that:-

(i). Most tests of specific components of the stomatal model do not have great impacts, with most cases showing changes in mean Vg of less than 10%

(ii). The exceptions were site specific; for example, SMD and, to a lesser extent, VPD had a significant effects on Vg at the Portuguese location

(iii). Although temperature overall had little effect on Vg, this was because of counterbalancing effects of direct limitation of g_s and indirect limitation through VPD, both of which individually were more sensitive.

(iv) The use of grid-scale 50m meteorological data leads to systematic overestimates of Ra compared with the use a sub-grid transfer function for different vegetation types

(v) Vg is consistently sensitive to variation in LAI.

It is important to note that the sensitivity analysis did not formally incorporate variation in the non-stomatal component of deposition. However, the important contribution of this component to seasonal mean deposition rates means that the major uncertainties in this part of the model parameterisation do need further attention

6. CONCLUSIONS

The work presented within this report has made significant progress towards developing an ozone deposition module for use within the EMEP photo-oxidant model. This model improves upon the relatively simple methods previously used to describe ozone deposition by the inclusion of physical and biological land-cover specific characteristics in combination with specific environmental factors that are known to influence ozone deposition to vegetated surfaces. This report has summarised the modifications and additions which were made to convert a single leaf based stomatal ozone flux model into a canopy based deposition model calculating atmospheric ozone loss via uptake both by the canopy leaves as well as to external vegetated and non-vegetated surfaces.

Preliminary deposition model runs were analysed to indicate the spatial and temporal variability in ozone deposition for different land cover-types and the relative contribution of the stomatal and non-stomatal deposition components. The results showed that deposition velocities varied both seasonally and diurnally with higher deposition velocities occurring during the summer months and during the middle of the day. Analysis of the component model results showed that these higher deposition velocities generally resulted from high canopy conductances and associated high stomatal ozone uptake. Although the highest deposition velocities were associated with high stomatal conductance the non-stomatal deposition pathways comprised a significant proportion of total deposition when considered over the entire growing season. The aerodynamic and boundary layer resistances were small compared to canopy resistance during the growing season, although for some short vegetation types (e.g. temperate cereals) the overall annual contribution of the sum of these two resistances to total resistance could approach 50%. For most land-cover types, temperature was found to cause the greatest limitation to stomatal deposition averaged over the year; irradiance and phenology were also important but to a lesser extent. The relative importance of the influence of different environmental variables on stomatal flux and hence ozone uptake varied by geographical region.

The performance of the deposition model was evaluated through a) comparisons with published data in the literature and b) direct comparisons with field data. The model produced deposition velocity estimates that were broadly consistent with the range

reported in the literature. The model was capable of predicting seasonal and diurnal patterns of deposition velocity, and provided realistic estimates of the relative contributions of stomatal and non-stomatal components.

More detailed comparisons with field data indicated that a) the model can predict the main features of deposition to subarctic pine forests but that predictions are highly sensitive to leaf area index values (Tuovinen, 2000); b) that the model can reproduce the broad diurnal patterns of stomatal conductance and ozone flux to current year needles of Norway spruce in Austria (Emberson et al. 2000c) and c) that while the model reproduced the major patterns of stomatal conductance and ozone flux in chamber experiments with Norway spruce, the model parameterisation could be further improved by taking into account interactive effects of soil moisture deficit and vapour pressure deficit and longer-term effects of soil moisture deficit (Karlsson et al., 2000). Interpretation of these findings should take into account the fact that the model parameterisation, designed for application across Europe, may not be appropriate for an individual field site. Once allowance has been made for local parameterisation, the model in general provides good agreement with field measurements of deposition and flux.

A sensitivity analysis of the model including the influence of soil moisture deficit (SMD) on deposition, was conducted for the four different locations across Europe (Simpson et al. in press). This showed that predictions of deposition velocity were relatively insensitive to most specific components of the stomatal model. The exceptions, primarily for the southern site, were soil moisture deficit and, to a lesser extent vapour pressure deficit. Furthermore, the limited sensitivity to temperature was due to counterbalancing of two stronger effects (a direct effect of low temperature and an indirect effect of high temperature through vapour pressure deficit). Scale effects on aerodynamic resistance and a strong effect of leaf area index (LAI) were also identified.

Two specific components of the model were identified as being in need of further research and development. The first of these was SMD. An evaluation of the performance of the SMD component of the model was performed for temperate cereal crops. The SMD model provided predictions which were consistent with those of the MORECS UK Meteorological Office model, and which appeared significantly better than those made using a model described by Mintz & Walker (1993). Estimations of SMD for different types of land-cover, and the associated effect on stomatal conductance, found that the limiting influence of SMD on g_s was stronger for root crops and deciduous forests than for cereal crops and coniferous forests. The accumulated SMD was greatest during July and August. This resulted in significant SMD related limitations to stomatal flux only occurring for those species whose growing seasons spanned this period. Remaining uncertainties with the SMD model include its parameterisation for use in a pan-European model, in particular over the selection of appropriate values of rooting depth for different land-cover types and available soil water values for different soil textures.

The second model component investigated in more detail was the parameterisation and implementation of LAI. Uncertainties associated with the simple canopy up-scaling algorithm were investigated and it was found that assigning vegetation-specific extinction coefficients could significantly alter canopy conductance estimates. Further, the use of an integrated rather than a “big leaf” canopy up-scaling approach should be applied when estimating conductances for canopies with LAI greater than 6 m^2/m^2. It is recognised that LAI will vary within species/cover types across Europe according prevailing climatic conditions. The potential for using satellite remote sensed data to provide information on

the spatial and seasonal variations in LAI across Europe was investigated. It was concluded that whilst such data may help in a qualitative sense to improve the parameterisation of LAI, a number of problems mean that remotely sensed data cannot be used routinely to estimate LAI through standard algorithms.

In summary, the research presented in this report has succeeded in developing an improved and more mechanistic ozone deposition model for application within the EMEP model. This model will also enable pan-European risk assessments for ozone impacts on vegetation to be based on stomatal ozone flux rather than AOT40. Hence, the model developed under this contract provides the basis for future consideration, within a consistent mechanistic framework, of both the broad patterns of ozone deposition across the landscape and its impact on ozone concentrations, and the stomatal flux of ozone to small areas of high sensitivity. The new model shows reasonable agreement with both primary field data and literature on ozone deposition. However, additional research is required to further test and improve the model, and to provide a stronger link to impacts on vegetation. Such improvements are essential to ensure that the model becomes an accepted tool for future assessments of ozone control policy within the UN/ECE framework.

7. FURTHER RESEARCH

Priorities for further research include testing and validating the model performance for as many land-cover types as possible. This work is an essential pre-requisite to acceptance of the deposition and stomatal flux models as tools for policy evaluation. To achieve these detailed validations, site-specific comparisons of the model predictions with field measurements collected from micrometeorological studies should be performed. These will test not only the ability of the model to predict deposition velocities but also to separate the stomatal and non-stomatal components of ozone deposition.

The results of these validation exercises can provide the basis for further modification of the deposition and stomatal flux models, both in terms of model formulation and model parameterisation, to improve predictions. Additional data should also be collected to improve the stomatal conductance database especially for species whose stomatal conductance database is less well defined. The database should also be extended to include additional crop species thereby increasing the number of species for which ozone effects modelling can be performed. For tree species, the focus should be on improving on existing stomatal conductance parameterisation of species for which modelling is currently performed e.g. Norway spruce, Scots pine, various oak species, beech, birch Allepo pine, Maritime pine and fir species. Data should also be collected that would enable the estimation of the length and timing of species / cover type specific growing seasons e.g. through the use of appropriate thermal time models.

The model should be modified to allow consistent parameterisation of LAI for both deposition (for which leaf area per unit land area is important) and stomatal flux, related to impacts (for which leaf area per unit vegetated area is important). This distinction is important in many areas of Europe, where vegetation cover is sparse. In addition, stomatal flux modelling should be modified to calculate total stomatal flux to the entire canopy as well as to single leaves in the upper canopy. This would enable the utilisation of flux-effect relationships which have been developed both using measured flux to the whole canopy (e.g Fuhrer et al. 1992) and by modelling flux to upper canopy leaves (e.g. Pleijel et al. 2000). In order to achieve these aims the land-cover database used within the deposition

modelling needs to be modified to describe the temporal and spatial climatic variation in LAI across Europe.

Although stomatal ozone flux has consistently been shown to be more related to impacts of ozone than external concentration or cumulative dose (e.g. AOT40), there are other factors which influence the sensitivity of vegetation to ozone. In particular, there is evidence that anti-oxidant systems, such as ascorbate, in the cell wall can reduce the amount of ozone reaching the primary site of damage, the cell membrane. There would thus be considerable value in assessing the feasibility of extending the model to include simulations of the extent of ozone scavenging in the cell wall, such as those of Plochl et al., (2000). In theory, this would provide a more comprehensive basis on which to model ozone impacts on vegetation, although this benefit would need to be weighed against the significant increase in model complexity and the problems of additional parameterisation.

The methods used to calculate soil moisture deficit should be further tested both with regards to the ability of the model to predict SMDs both temporally, (as described in terms of the preliminary assessment presented in this report) and spatially and for different land cover-types. The influence of SMD on species-specific stomatal conductance should also be further researched especially in relation to effective rooting depths and the respective SMD necessary to induce hormonal signals for stomatal closure. In addition, European data describing crop irrigation needs to be collected and applied within both the deposition and the stomatal flux models since the presence of irrigation will encourage stomatal opening thereby increasing the absorbed ozone dose.

The incorporation of the deposition and stomatal ozone flux modules within the EMEP photo-oxidant model needs to be performed in a way that is internally consistent. This should ensure that stomatal ozone flux to species not included in the ozone deposition model is predicted using the boundary layer ozone concentrations after deposition has been modelled. As such, the EMEP model should be set up to calculate ozone uptake separately from total deposition calculations to avoid “double counting” of the absorbed dose to vegetation. The resulting spatial patterns of deposition and stomatal flux across Europe should be assessed in terms of the implications for ozone impacts on vegetation and for modelling of pollutant concentrations and budgets. The findings should then be critically evaluated in terms of the implications in the context of policy issues relating to the control of ozone precursors.

Finally, the sensitivity of the model predictions should be assessed in the context of the uncertainties in model formulation and parameterisation, and in the underlying land-cover and meteorological databases.

8. DISSEMINATION OF RESULTS

8.1 Conference presentations

Throughout the course of this project, we have endeavoured to present the work at appropriate conferences and workshops, both to provide opportunities for critical assessment and comment, and to allow us to disseminate the work to relevant communities within UN/ECE. These have included:-

(i). annual workshops of ICP-vegetation; presentations are summarised below.

(ii). annual workshops of the ICP Mapping and Modelling group; presentations are summarised below

(iii). the Level II Critical Levels workshop in Gerzensee (Switzerland) in April 1999; presentations are summarised below

(iv). the Biatex workshop on surface-atmosphere exchange in Edinburgh in June 2000

(v). the UK CAPER meeting in Birmingham in April 2000

Verbal presentations

"Progress with Level II models" given by Dr. Lisa Emberson at the 13th Task Force Meeting of the ICP-Vegetation.

"Modifying the EMEP model for ozone and looking at impacts using the SEI landcover map" given by Dr. Lisa Emberson at the 16th Task Force Meeting of the ICP-Mapping.

“EMEP modelling of AOT40 (and ozone fluxes ?) across Europe – developments and possibilities” given by Dr. David Simpson at the Level II Critical Levels workshop in Gerzensee (Switzerland) in April 1999

“Development of flux models for level II mapping of ozone” given by Dr. Lisa Emberson at the Level II Critical Levels workshop in Gerzensee (Switzerland) in April 1999

“Flux modelling for ozone – from European scale to sub-grid” given by Dr. David Simpson at the Biatex workshop on surface-atmosphere exchange in Edinburgh in June 2000

“Comparisons of measured and modelled deposition to forests” given by Dr. J.-P. Tuovinen at the Biatex workshop on surface-atmosphere exchange in Edinburgh in June 2000

“Modelling of ozone flux and deposition to vegetation in Europe” given by Prof. M. R. Ashmore at the UK CAPER meeting in Birmingham in April 2000

Poster presentations (see Annexe for reproductions)

Emberson, L.D., Wieser, G. and Ashmore, M.R. Comparison of measured and modelled stomatal conductance and ozone flux for Norway spruce. Presented at the Level II Critical Levels workshop in Gerzensee (Switzerland) in April 1999

Emberson, L.D., Ashmore, M.R., Cambridge, H.M., Simpson, D., and Tuovinen, J.-P. Modelling ozone flux and deposition across Europe

Emberson, L.D., Ashmore, M.R., Simpson, D., Tuovinen, J.-P., and Cambridge, H.M., Modelling and mapping of stomatal uptake of ozone by European vegetation. Presented at 6th International conference on Air-Surface exchange of gases and particles. Edinburgh, Scotland

8.2. Written papers

All written outputs from the project are included in the project Annexe, and are listed separately in the Reference section below. These include peer-reviewed publication in scientific journals, conference papers and the EMEP report. This includes relevant publications by all five project co-ordinators. In addition, the Annexe includes scientific papers that are currently in press or under review and the two internal project reports on LAI and SMD.

8.3. Web-based outputs

The key features of the work have been presented also on the web pages of the Stockholm Environment Institute at York:-
http://www.york.ac.uk/inst/sei/ozone/about-atmos.htm

and the Environment Department at York University :-
http://www.york.ac.uk/depts/eeem/resource/emberson/emberson.htm

9. REFERENCES

Output References :-

Ashmore MR & Emberson LD (1999) Development of flux models for level II mapping of ozone. In: Critical Levels for Ozone – Level II (B Achermann & J Fuhrer eds.), pp. 37-40. SAEFL, Berne.

Baumgarten M, Werner H, Haberle K-H, Emberson LD, Fabian P & Matyssek R (2000). Seasonal ozone response of mature beech trees (Fagus sylvatica) at high altitude in the Bavarian forest (Germany) in comparison with young beech grown in the field and phytotrons. Environmental Pollution, 109, 431-442.

Emberson LD, Ashmore MR, Cambridge HM, Simpson D & Tuovinen J-P (1999). Modelling ozone flux and deposition across Europe. In: Critical Levels for Ozone – level II (B Achermann & J Fuhrer, eds.), pp. 289-292. SAEFL, Berne.

Emberson LD, Wieser, G., and Ashmore MR. (1999). Comparison of measured and modelled stomatal conductance and ozone flux for Norway spruce. In: Critical Levels for Ozone – level II (B Achermann & J Fuhrer, eds.), pp. 293-296. SAEFL, Berne.

Emberson, L., Ashmore, M.R., and Cambridge, H.M. Simpson, D. and Tuovinen, J.P. (2000a) Modelling stomatal ozone flux across Europe, Environmental Pollution, 109, 403-414

Emberson LD, Wieser G & Ashmore MR (2000b). Modelling of stomatal conductance and ozone flux of Norway spruce: comparison with field data. Environmental Pollution, 109, 393-402

Emberson, L.D., Simpson, D.S., Tuovinen, J.-P., Ashmore, M.R. and Cambridge, H.M. (2000c) Towards a model of ozone deposition and stomatal uptake over Europe. Norwegian Meteorological Institute, Oslo, EMEP MSC-W Note X/00.

Emberson, L.D., Ashmore, M.R., Simpson, D., Tuovinen, J.-P., and Cambridge, H. (in Press) Modelling and mapping ozone deposition in Europe. Water, Air and Soil Pollution

Simpson D, Emberson LD, Ashmore MR, Cambridge HM & Tuovinen J-P (1999). EMEP modelling of AOT40 (and ozone fluxes?) across Europe – developments and possibilities. In: Critical Levels for Ozone – Level II (B Achermann & J Fuhrer, eds)., pp. 35-36. SAEFL, Berne.

Simpson D, Tuovinen J-P, Emberson LD & Ashmore MR (in press). Characteristics of a sub-grid ozone deposition and flux model. Water Air and Soil Pollution

Tuovinen J-P (2000). Assessing vegetation exposure to ozone: properties of the AOT40 index and modifications by deposition modelling. Environmental Pollution, 109, 361-372.

Tuovinen J-P, Emberson LD, Simpson D, Ashmore MR, Aurela M & Cambridge HM (2000a). A new dry deposition module for ozone – comparisons with measurements. Proceedings of the Eurotrac Symposium 2000 Garmish-Partenkirchen (in press)

Tuovinen J-P, Simpson F, Mikkelson T, Embersom LD, Ashmore MR, Aurela M, Canbridge HM, Hovmand M, Jensen NJ, Laurila T, Pilegaard K & Ro-Poulsen H (in press) Comparisons of measured and modelled deposition to forests in Northern Europe. Water, Air and Soil Pollution

Report References :

Baldocchi, D.D., Hicks, B.B. and Camara, P. (1987) A canopy stomatal resistance model for gaseous deposition to vegetated surfaces. Atmos. Environ. 21: 91-101

Brook, J.R., Zhang,L., Li, Y., Johnson, D. (1999) Description and evaluation of a model of deposition velocities for routine estimatesof dry deposition over North America. Part II: review of past measurements and model results. Atmospheric Environment 33: 5053-5070

Caldwell, M.M., Meister, H.-P., Tenhunen, J.D. and Lange, O.L. (1986) Canopy structure, light microclimate and leaf gas exchange of Quercus coccifera L. in a Portuguese macchia: measurements in different canopy layers and simulations with a canopy model. Trees 1:25-41

Canadell, J., Jackson, R.B., Ehleringer, J.R., Mooney, H.A., Sala, O.E., Shulze, E.-D. (1996) Maximum rooting depth of vegetation types at the global scale. Oecologia 108: 583-595

Cieslik, S. and Labatut, A. (1997) Ozone and heat fluxes over a Mediterranean Pseudostepe. Atmos. Env. 31: 177-184

Coe, H., Gallagher, M.W., Choularton, T.W. and Dore, C. (1995) Canopy scale measurements of stomatal and cuticular O_3 uptake by Sitka spruce. Atmos. Environ. 29: 1413-1423

CCCP (1991) Land Use Map of the Former USSR, (1:4000000) Moscow

Davies, W.J., Tardieu, F., and Trejo, C.L. (1994) How do chemical signals work in plants that grow in drying soil ? Plant Physiology 104: 309-314

Emberson (1997) Defining and mapping relative potential sensitivity of European vegetation to ozone. Ph.D. Thesis, Imperial College, University of London.

ESA (1992) Remote sensing map of Europe (1:6,000,000). European Space Agency / ESTEC, Noordijk.

Eurostat (1994) Crop Production Statistics. Office for Official Publications of the European Communities, Brussels.

FAO-Cartographia, (1980) Land use map of Europe (1:2,500,000) Cartographia, Budapest

FAO-Agristat (1990) FAO Vol. 1, United Nations

Fowler, D., Flechard, C., Coyle, M. and Storeton-West, R. (1999) Ozone fluxes to vegetation in the field, separating stomatal from non-stomatal uptake. In: J. Fuhrer and B. Achermann (Eds.), Critical Levels for Ozone – Level II. Environmental Documentation No. 115. Swiss Agency for Environment, Forest and Landscape, Bern, Switzerland, pp. 279-287

Goward, S.N. and Huemmerich, K.F. 1992. Vegetation canopy PAR absorptance and the nornmalised difference vegetation index: An assessment using the SAIL model. Remote Sensing of the Environment. **39** 119-140.

Grimm, G.A. and Fuhrer, J. (1992). The response of spring wheat (*Triticum aestivum* L.) to ozone at higher elevations. I Measurement of ozone and carbon dioxide fluxes in open-top field chambers. New Phytol. Vol. 121 pp. 201-210

Grünhage, L., Dämmgen, U., Haenel, H.-D. and Jäger, H.-J. (1994) Response of a grassland ecosystem to air pollutants: III – The chemical climate: vertical flux densities of gaseous species in the atmosphere near the ground. Environ. Pollut. 85: 43-49

Hosker, R.P., Jr. (1986) Practical Application of Air Pollutant deposition Models – Current status, data requirements and research needs. In: Air Pollutants and their Effects of the Terrestrial Ecosystem. Legge, A.H. and Krupa, S.V. (Eds.) John Wiley, New York pp. 505-567

Jackson, R.B., Canadell, J., Ehleringer, J.R., Mooney, H.A., Sala, O.E., Schulze, E.D. (1996) A global analysis of root distributions for terrestrial biomes. Oecologia 108: 389-411

Jakobsen, H.A., Jonson, J.E., and Berge, E. (1996) Transport and deposition calculations of sulphur and nitrogen compounds in Europe for 1992 in the 50 km grid square by use of the multi-layerEulerian model. EMEP/MSC-W Report 2/96. The Norwegian Meteorological Institute, Oslo, Norway.

Jones, H.G. (1992) Plants and Microclimate: A Quantitative Approach to Environmental Plant Physiology. 2nd edition. Cambridge University Press, Cambridge.

Jonson, J.E., Tarrason, L: and Sundet, J., (1999) Calculation of ozone and other pollutants for the summer of 1996. Environmental Management and Health, **10**, 245-257

Karlsson, P.E., Pleijel, H., Pihl Karlsson, G., Medin, E.L. and Skärby, L. (2000) Simulations of stomatal conductance and ozone uptake to Norway spruce saplings in open-top chambers. Environmental Pollution 109: 443-451

Korner, C. (1994). Leaf diffusive conductances in the major vegetation types of the globe. In: E.D. Schulze. and Caldwell, M.M. (eds.) Ecophysiology of Photosynthesis. Ecological Studies 100. Springer, Berlin Heidelberg New York, pp. 463-490

Magnani, F., Leonardi, S., Tognetti,R., Grace, J. and Borghetti, M. (1998) Modeling the surface conductance of a broad-leaf canopy: effects of partial decoupling from the atmosphere. Plant, Cell and Environment. 21: 867-879

de Miguel, A. and Bilbao, J. (1999) Ozone dry deposition and resistances onto green grassland in summer in central Spain. J. Atmos. Chem. 34: 321-338

Mintz, Y., and Walker, G. (1993) Global fields of soil moisture and land surface evapotranspiration derived from observed precipitation and surface air temperature. Journal of Applied Meteorology 32: 1305-1334

Montieth, J.L. and Unsworth, M.H. (1990) Principles of Environmental Physics. Arnold, London.

Norman, J.M. (1982) Simulation of microclimates, In: Biometeorology in integrated pest management (ed. Hatfield, J.L. & Thompson, I.J.) pp. 65-99. Academic Press, New York.

Pilegaard, K., Jensen, N.O. and Hummelshøj, P. (1995a) Seasonal and diurnal variation in the deposition velocity of ozone over a spruce forest in Denmark. Water Air Soil Pollut. 85: 2223-2228

Pilegaard, K., Jensen, N.O. and Hummelshøj, P. (1995b) Deposition of nitrogen oxides and ozone to Danish forest sites. In: G.J. Heij and J.W. Erisman (Eds.), Acid Rain Research: Do we have enough answers?, Elsevier Science, pp. 31-40

Pilegaard, K., Hummelshøj, P., Jensen, N.O., Kristensen, L. (1997) Measurements of fluxes of particles, ozone, nitrogen oxides and carbon dioxide to coniferous and deciduous forests. In: S. Slanina (Ed.), Biosphere-Atmosphere Exchange of Pollutants and Trace Substances, Springer, Berlin, pp. 391-396

Pleijel, H., Danielsson, H., Gelang, J., Sild, E., and Sellden, G. (1996) Growth stage dependance of the grain yield response to ozone in spring wheat. In: Knoflacher, M., Schneider, J., and Soja, G. (eds.) Exceedance of Critical Loads and Levels; Umbweltbundesamt, Vienna, 22-24 Nov. 1996.

van Pul, W.A.J. and Jacobs, A.F.G. (1994) The conductance of a maize crop and the underlying soil to ozone under various environmental conditions. Boundary-Layer Meteorology 69:83-99

Sandnes Lenschow, H. and Tsyro, S. (2000) Meteorological input data for EMEP / MSC-W air pollution models. Technical Report EMEP MSC-W Note 2/98, The Norwegian Meteorological Institute, Oslo.

Simpson, D. (1996) Modelled data in relation to AOT40. In: Critical levels for ozone in Euorpe: Testing and finalizing the conepts. Kärenlampi, L. and Skärby, L. (Eds.) (UN/ECE Workshop Report). University of Kuopio, Dept. of Ecology and Environmental Science, Kuopio, Finland.

Sellers, P.J., Tucker, C.J., Collatz, G.J. Los, S.O., Justice, C.O., Dazlich, D.A, and Randall, D.A. 1994. A global 1 degree by 1 degree data set for climate studies. Part 2: the generation of global fields of terrestrial biophysical parameters from NDVI. International Journal of remote Sensing. Vol. 15. No 17. pp3519-3545.

Slovik, S., Siegmund, A., Führer, H.-W. and Heber, U. (1996) Stomatal uptake of SO_2, NO_x and O_3 by spruce crowns (*Picea abies*) and canopy damage in central Europe. New. Phytol. 132: 661-676

Sturm, N., Köstner, B., Hartung, W., Tenhunen, J.D. (1998) Environmental and endogenous controls on leaf- and stand-level water conductance in a Scots pine plantation. Ann. Sci. For. 55: 237-253

Tuovinen, J.-P., Aurela, M. and Laurila, T. (1999) Measured and modelled ozone deposition to three different ecosystems in Finland. In: P.M. Borrell and P. Borrell (Eds.), Proceedings of EUROTRAC Symposium ’98, WITpress, Southampton, UK, pp. 197-201